

Spatio-temporal distribution of major and trace metals in estuarine sediments of Dhamra, Bay of Bengal, India—its environmental significance

D. R. Satapathy · C. R. Panda

Received: 22 April 2014 / Accepted: 28 October 2014 / Published online: 6 December 2014
© Springer International Publishing Switzerland 2014

Abstract The research depicts the spatial and temporal variation of major and trace metals in marine sediments at various monitoring stations of Dhamra estuary, Bay of Bengal, Odisha. The concentration and distribution of selected metals in surface sediments of the estuary were studied in order to assess the spatial extent of anthropogenic inputs viz., mining activities and to estimate the effects of seasonal variations on geochemical processes in this particular tropical estuarine system. Surface sediments reflect the presence of trace and major metals in parts per million, and the concentrations vary in the range of Cu (0.083 to 127.2), Ni (17.35 to 122.8), Co (1.2 to 31.58), Pb (0.8 to 95.86), Zn (12.1 to 415), Cd (0 to 11) and Cr (35.21 to 5,890), Fe (7,490 and 169,100), Mn (20 to 69,188), Ca (10 to 10,520), Mg (990 to 28,750), Na (300 to 51,700), and K (1,100 to 30,010). The comparison of spatial distribution of metal contents using GIS in marine sediments indicates that there is a substantial anthropogenic input in the Dhamra estuary. The enrichment of Cr is ascribed to the sedimentation of Brahmani River, passing through the mining region and discharging Cr pollutant to the sea. Similarly, the

sources of Cd are attributable to corrosion-resistant paints used by a large number of trawlers. Contamination factor has been calculated for various metals to assess the degree of pollution. As per Hakanson's classification, Cr indicates very high contamination with considerable contamination of Cd, whereas moderate contamination of Pb, Zn, and Mn are observed in marine sediments. Pollution load index also indicate that there is deterioration of site quality in premonsoon season, which almost attains the baseline level in post monsoon and perfection in monsoon season (Tomlinson et al. (*Helgolander Wissenschaftliche Meeresuntersuchungen*, 33, 566–572, 1980)). The geoaccumulation index shows that the metal concentrations in sediments can be considered as background levels except Cr and Cd. The geoaccumulation index shows that Cr is moderately contaminated and it is higher in offshore region in post monsoon and monsoon than premonsoon season. All the calculated indices show that Cr and Cd levels are more than the desired limits in the marine sediments. Multivariate statistical analysis evaluates the plausible sources of contaminants, attributing to mining, industrial, and urban wastes by way of Brahmani River discharging to the estuarine region.

D. R. Satapathy (✉) · C. R. Panda
Environment and Sustainability Department, CSIR-Institute
of Minerals and Materials Technology,
Bhubaneswar 751013 Odisha, India
e-mail: drsatapathy@immt.res.in

D. R. Satapathy
e-mail: drsatapathy@gmail.com

Keywords GIS · Pollution dispersion · Estuarine sedimentation · Heavy metals · Geoaccumulation index · Pollution load index

Introduction

Estuaries form a transition zone between river and ocean environments, which are subjected to marine and river influences. As a result, estuaries are suffering from degradation by many factors, including sedimentation from soil erosion, deforestation, overgrazing, poor farming practices, overfishing, drainage of sewage and industrial wastes, filling of wetlands, eutrophication due to excessive nutrients from sewage and animal wastes, and pollutants including heavy metals, radionuclides, and hydrocarbons (Wolanski 2007). Thus, estuaries are prone to various anthropogenic activities causing threat to marine ecosystem and mankind. Hence, it is essential to identify the environmental consequences in the estuaries which are vulnerable due to substantial industrial development and in turn resulting urban developments. Sediments are preferable monitoring ‘tools’ since contaminant concentrations are of higher magnitude and they show less variation in time and space, allowing more consistent assessment of spatial and temporal contamination (Tuncer et al. 2001; Beiras et al. 2003; Caccia et al. 2003). Sediment studies play an important role in assessments of pollution status of marine environment (Pekey 2006). River systems are a present-day health indicator of cities, which includes the biochemical and physico-chemical components generated from both natural and anthropogenic processes. In developing countries, the lack of reliable and frequent available data required for modeling such scenarios is an acute problem Roy and Katpatal (2011).

Sediments, especially finer fractions, can adsorb contaminants from sea water and exert a strong influence on the transport and ultimate distribution of contaminants (Richard et al. 2001). Hence, it is a significant aspect to know the spatial extent to which sediment characteristics especially the size fractions can change due to the influence of both anthropogenic and natural factors causing potential impacts on pollution. In order to measure the occurrence and spatial distribution of toxic substances, further understanding on the role of human activities in releasing contaminants to the environment is required. This information aids for devising effective strategies to mitigate deleterious health effects.

Various geospatial tools viz., geographic information system (GIS), remote sensing (RS), and Global Positioning System (GPS) form an effective planning tool and a sound basis for continued coastal monitoring (O'Regan 1996; Stanbury and Starr 1999). Using a GPS

receiver for field sampling allows inclusion in a GIS platform for subsequent analytical, statistical, and modeling analyses. Environmental scientists are expected to provide interpretations about patterns across broad scales of space and time but face the challenge that the environment can vary at smaller spatial scales than commonly recognized (Elsdon and Connell 2009). The aims of the investigation presented in this paper are (a) to integrate the geospatial technologies with other sediment environmental parameters viz., trace and major metal contents, size fraction, organic carbon, for the estimation of index imparting assessment of pollution behavior into a GIS environment using Dhamra estuary as a case study site, (b) to identify plausible sources and the dominant direction of transport of major and trace metals in sediments in Dhamra estuary, and (c) to derive information on the spatial distribution and its relation to particulate size distribution and total organic carbon. The derived information on spatial and temporal variability could be well utilized for appropriate monitoring as well as management practices.

The study area

The Dhamra estuary is a tropical estuary on the East Coast of India and its hydrological characteristics are governed by the monsoon regime. It is situated on the east coast of India within 86° 57' 00" E–87° 01' 00" E and 20° 45' 00" N–20° 48' 00" N being sheltered between the main land mass and the Kanika Sand Island on the eastern side. The Dhamra River receives indiscriminate waste discharges from two major rivers viz., Brahmani and Baitarani, which are in close proximity to the mineral belt of Odisha, Jharkhand and West Bengal, and the mining activities in this region may influence the biological and geochemical conditions of the estuarine waters to a considerable extent.

The state of Odisha has a coastline of 480 km, and one of the most dynamic coastal environments in India due to its location and physical factors especially its network of large, powerful rivers with their delta and estuarine systems, each with a variety of ecological niches and habitats. The area includes Bhitarkanika Wildlife Sanctuary and Gahirmatha Marine Sanctuary, which are of international repute being environmentally sensitive areas. The Gahirmatha beach located in the Bhitarkanika Wildlife Sanctuary supports the largest known nesting ground of olive ridley turtle in the world

(Bustard and Kar 1981; Dash and Kar 1990). About 0.2 to 0.7 million olive ridley turtles visit this beach during December to April for mass nesting every year. However, in the last 20 years, large-scale mortality and shifting of nesting are being observed. The newly constructed open-sea Dhamra port being located near the Bhitarkanika National Park and Gahirmatha Marine sanctuary is of great concern due to its operation and ancillary development, viz., continual dredging of the channel, which may have possible harmful impacts on marine environment.

Geological and oceanographic environment

Lithogenic sediments (clayey silts/silty clays) are predominant on the continental margins and in the region. The clay fraction of the Bay of Bengal is mainly composed of chlorite, illite, mixed-layer smectite, and kaolinite. The climatic condition in the source area is humid to arid. Sea currents and circulation patterns are generally wind driven, as a result of which the Bay of Bengal experiences severe cyclone during September to December affecting Eastern India. During monsoons, these rivers carry sediment load which is many times more than their normal load. The sediments are carried from their point of origin to the local stream network commonly by mass-weathering processes, typically soil creep. Thus, contaminants from various point and non-point sources are mixed with the sediments and eventually become part of the stream load, causing the estuary to be polluted due to geogenic and anthropogenic factors.

Study design and methodological approach

Environmental monitoring is used in the baseline data creation, impact assessments, as well as cases in which human involvement carry a risk of harmful effects on the natural environment. All monitoring strategies are often designed to establish the current status of an environment or to establish trends in environmental parameters.

Sediment sampling

Sampling was carried out on monthly basis for a period of 2 years from May 2009 to March 2011. However, the data are presented as clustered values ranging

premonsoon (February–May), monsoon (June–September), and post monsoon (October–January) seasons. Sediment samples were collected from the upper surface using a Van veen grab from eight stations in the Dhamra estuary (Fig. 1) covering a distance of around 35 km from the shoreline during field campaigns in the vessel. The overall sediment pattern in the study area is not regarded as uniform throughout the year, and therefore the collected surface samples were assumed to be representative of different seasonal weather conditions.

Sediment analysis

The samples thus collected have undergone analysis for different parameters, viz., major and trace metals content, size fraction, and total organic carbon content.

Major and trace metal analysis

The sediments were dried at 50–60 °C in an oven and disaggregated in an agate mortar before chemical treatment. The powdered samples were digested in triplicate in 100 ml Teflon beaker followed by addition of 2 ml of HClO₄, 12 ml of HF, and 8 ml of HNO₃. The residue was dissolved in concentrated HCl and diluted to 25 ml (Tessier et al. 1979). Chemicals of high purity (Merck, Germany) were used, and standard solutions were prepared from 1,000 mg/l stock solution of each metal. Then the concentration of metals was measured using an atomic absorption spectrophotometer (AAS, Shimadzu, AA-7000). The accuracy of the analytical procedures was assessed using the certified reference material BCR®-277R (BCR is the European Community Bureau of Reference, now known as the Standards, Measurements, and Testing Program) and yielded results within the reference value range (Flanagan 1973).

Particle size analysis

The sediment classification used here is that of Shepard's (1954) classification with the sand, silt, and clay boundaries based on the Wentworth (1922) scale. Thus, sand, silt, and clay fractions are composed of particles whose diameters range from 2,000 to 62.5, 62.5 to 3.91, and less than 3.91 μm, respectively. Based on the relative abundance (wt.%) of each size class, the sediment texture was determined according to the classification of Shepard (1954). The threshold limit

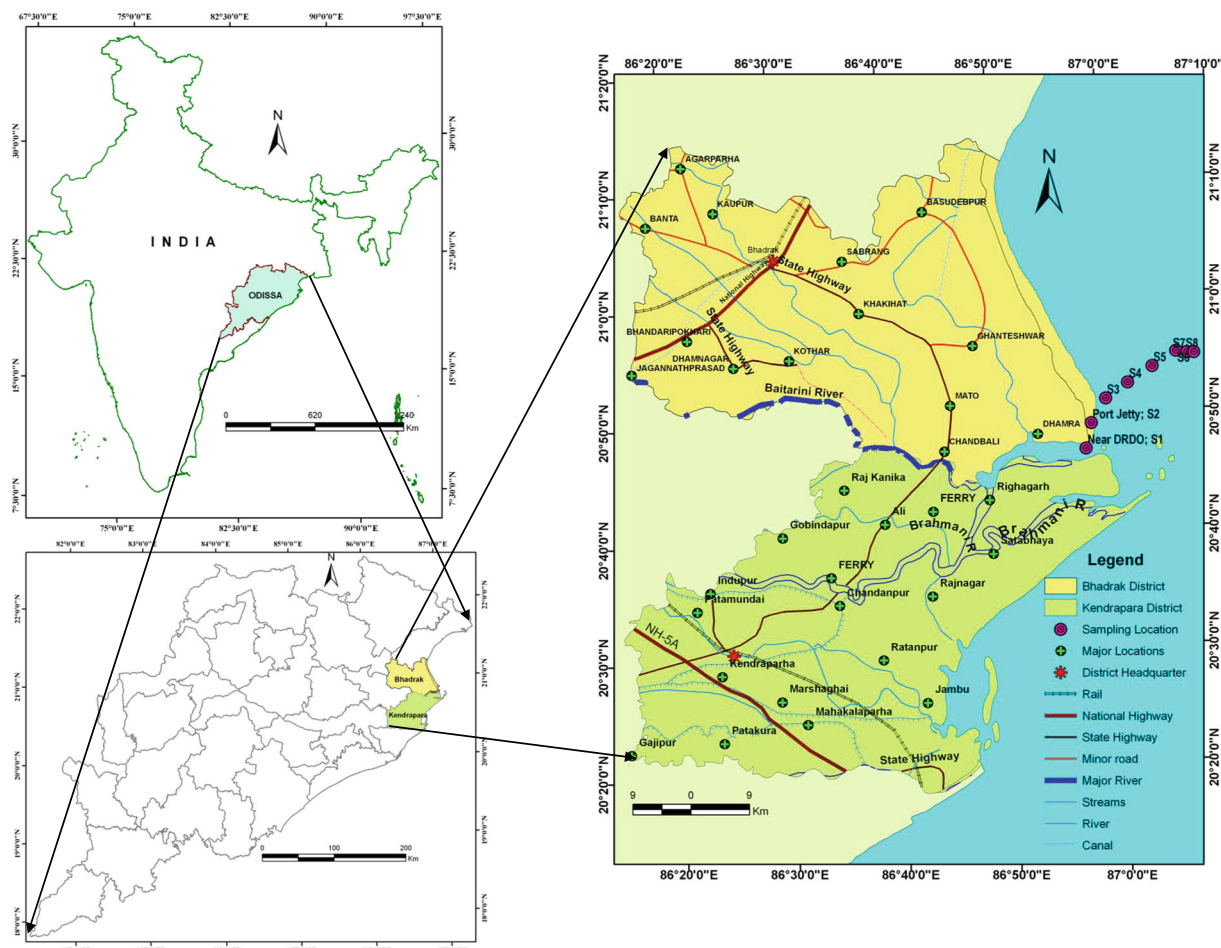


Fig. 1 Study area depicting sampling locations in Dhamra estuary, Bay of Bengal, India

between clay and silt has been simulated at 4 μm and silt and sand content at 63 μm . The classification is applied regardless of sediment type and origin.

Coarse fraction analysis The sample is wet sieved through a 63- μm sieve to separate the sample into coarse (sand and gravel which are retained on the sieve) and fine (clay and silt) fractions. Distilled water was used during wet sieving supposing that the fine fraction comprises greater than 5 % of the sample.

Fine fraction analysis The fine-grained fraction of the sediment is defined as silt (particles with diameters less than 63 μm down to 4 μm) plus clay (particles with diameters less than 4 μm , with colloidal clay being less than 0.1 μm). Because of their small size, fine-fraction particles are

difficult to measure by sieving. Therefore, the classical techniques to analyze the fine-grained portion of grain-size distributions are dominated by sedimentation methods like the hydrometer and pipette methods. These methods had been adopted to determine the texture of sediment condition. Then the different grain size fractions were analyzed by weight sieving and pipette method (Lewis 1984), and the results were expressed in weight percentage. The results are represented in the Shepard's texture diagram.

Organic carbon

The organic carbon (OC) was determined by exothermic heating and oxidation with potassium dichromate and concentrated H_2SO_4 , followed by titration of excess

dichromate, with 0.5 N of ferrous ammonium sulfate solutions (Gaudette et al. 1974).

Methods for evaluating the pollution impact

There are a number of numerical methods which are being used for quantifying the degree or level of metal contamination in sediments. Various authors (Salomons and Forstner 1984; Muller 1969; Hakanson 1980) have proposed pollution impact scales or ranges to convert the calculated numerical results into broad descriptive intervals of pollution ranging from low to high intensity.

Enrichment factor

A number of different enrichment calculation methods have been adopted to find out if there was enrichment relative to the local baseline data. Hence, metal contamination in sediments requires pre-anthropogenic knowledge of metal concentrations as pristine or background values. Many anthropogenic activities including drainage run-off attribute towards heavy metal enrichment.

The enrichment factor (EF) was evaluated to assess the degree of contamination as well as for better understanding of the distribution of the elements of anthropogenic origin (Simex and Helz 1981). The EF method normalizes the measured heavy metal content with respect to a sample reference metal such as Fe or Al (Ravichandran et al. 1995). Sharma et al. (1999) used both Al and Fe to distinguish natural and anthropogenic sources in recent sediments from Texas estuaries. In the current study, Fe was chosen for normalizing element while determining EF values (Baut and Chesselet 1979) and is one of the widely used reference element (Chakravarty and Patgiri 2009; Seshan et al. 2010). The EF is calculated as follows:

$$\text{Enrichment factor} = \frac{C_n(\text{sample})/C_{\text{ref}}(\text{sample})}{B_n(\text{background})/B_{\text{ref}}(\text{background})}$$

where C_n is the concentration of n th element and B_n is the background value of n th element in average shale (Turekian and Wedepohl 1961). Elements which are naturally derived have an EF value of nearly unity, whereas elements of anthropogenic origin may be sliced into different EF values. Basically, six categories are recognized and widely published: (a) <1 background concentration, (b) 1–2 depletion to minimal enrichment, (c) 2–5 moderate enrichment, (d) 5–20 significant enrichment, (e) 20–40 very high enrichment, and (f) >40

extremely high enrichment (Sutherland 2000). In the present study, Fe has been considered as reference element to assess the enrichment in sediments.

Contamination factor

The level of contamination of sediments by metal is expressed in terms of a contamination factor (CF) which is calculated as (Hakanson 1980):

$$C_f^i = \frac{[C_0^i - 1]}{C_n^i}$$

where C_f^i is the contamination factor, $C_0^i - 1$ is the mean content of metals from at least five sampling locations, and C_n^i is the concentration of elements in the earth's crust as a reference value. The CF is broadly divided into four significant categories, viz., the contamination factor $CF < 1$ refers to low contamination; $1 \leq CF < 3$ means moderate contamination; $3 \leq CF \leq 6$ indicates considerable contamination and $CF > 6$ indicates very high contamination (Hakanson 1980; Aksu et al. 1998; Nasr et al. 2006).

Pollution load index

The pollution level for each site was evaluated by adopting pollution load index (PLI) developed by Tomlinson et al. 1980:

$$CF = C_{\text{Metal}} / C_{\text{Background}}$$

$$PLI = \sqrt[n]{(CF_1 \times CF_2 \times CF_3 \times \dots \times CF_n)}$$

where CF is the contamination factor, n is the number of metals, C_{metal} is the metal concentration in polluted sediment, and $C_{\text{Background}}$ is the background value of that metal. In the current study, it has been found to be appropriate to express the PLI as the geometric mean of

Table 1 The I_{geo} classes with respect to sediment quality

I_{geovalue}	I_{geoclass}	Designation of sediment quality
>5	6	Extremely polluted
4–5	5	Strongly to extremely polluted
3–4	4	Strongly polluted
2–3	3	Moderately to strongly polluted
1–2	2	Moderately polluted
0–1	1	Unpolluted to moderately polluted
0	0	Unpolluted

Table 2 Statistics of trace metals (ppm) in marine sediment at Dharmra

Location	Season	Statistics	Cu	Ni		Co		Zn
			Bulk	-63 μm	Bulk	-63 μm	Bulk	-63 μm
S1	Premonsoon	Range (min, max)	(12.8, 33.6)	(18, 56.5)	(42.4, 55)	(49.8, 71.8)	(11.5, 23.7)	(43, 75.8)
	Monsoon	Mean±std dev	24.56±8.64	44.41±17.80	47.05±5.62	60.26±11.18	26.65±5.25	61.03±14.11
	Post monsoon	Range (min, max)	(4.9, 10.01)	(26.5, 33.4)	(27.9, 59.2)	(37.2, 68.9)	(1.2, 2.8)	(16, 19)
	Premonsoon	Mean±std dev	7.46±3.61	29.95±4.88	43.55±22.13	53.05±22.42	2.00±1.13	17.50±2.12
S2	Monsoon	Range (min, max)	(6.51, 17.8)	(20.4, 80.71)	(24.39, 48.5)	(41.7, 54.4)	(10.02, 13.4)	(24, 50.5)
	Post monsoon	Range (min, max)	11.33±4.71	41.45±27.82	37.30±10.22	48.13±5.39	11.43±1.51	35.98±11.29
	Premonsoon	Mean±std dev	(12.5, 42.75)	(11.6, 40.8)	(55.99, 101)	(21.03, 89.4)	(19.15, 8)	(27, 92.81)
	Monsoon	Range (min, max)	27.98±15.14	23.80±15.18	78.36±22.51	60.71±55.49	6.93±7.70	52.60±35.25
S3	Premonsoon	Range (min, max)	(0.083, 12.4)	(0.307, 41.4)	(20.4, 61.44)	(44.8, 50.8)	(8.4, 13.6)	(37.1, 84.8)
	Monsoon	Mean±std.dev	7.36±6.46	22.30±20.70	41.28±20.53	47.96±3.01	10.39±2.81	56.97±24.83
	Premonsoon	Range (min, max)	(4.1, 29.4)	(23.43, 35.06)	(33.8, 59.26)	(33.47, 63.74)	(14.3, 22.74)	(36.4, 71.1)
	Monsoon	Mean± std dev	22.44±10.38	29.92±4.91	49.66±10.47	50.70±12.11	18.21±3.89	19.87±5.21
S4	Premonsoon	Range (min, max)	(14.2, 43.78)	(15.2, 37.57)	(34.5, 70.03)	(53.6, 92.1)	(1.2, 15.8)	(43.9, 84.18)
	Monsoon	Mean± std dev	23.19±14.79	28.82±11.96	57.04±19.60	69.90±19.92	6.33±8.21	9.46±7.86
	Post monsoon	Range (min, max)	(0.188, 28.4)	(0.279, 39.4)	(38.57, 69.4)	(28.77, 47.6)	(15.62, 22.6)	(15.8, 24.29)
	Premonsoon	Mean± std dev	17.65±13.50	23.63±16.66	52.79±13.26	40.21±8.19	19.36±2.94	19.37±3.55
S5	Monsoon	Range (min, max)	(8.9, 42.62)	(21.5, 75.4)	(31.56, 72.26)	(46.5, 89.2)	(10.1, 21.5)	(13.7, 31.39)
	Premonsoon	Mean±std dev	24.05±11.86	44.65±18.43	51.06±16.21	67.90±14.07	15.56±4.42	22.66±6.04
	Monsoon	Range (min, max)	(12.50, 30.6)	(11.40, 38.9)	(45.75, 112.7)	(43.80, 51.2)	(1.60, 13.66)	(6.30, 13.06)
	Premonsoon	Mean±std dev	21.40±9.05	26.38±13.91	69.22±37.70	46.82±3.87	5.82±6.80	8.82±3.69
S6	Post monsoon	Range (min, max)	(0.33, 37.6)	(0.15, 40)	(35.70, 63.14)	(17.35, 63.61)	(14.00, 24.65)	(14.67, 21)
	Premonsoon	Mean±std dev	19.10±15.22	21.75±17.88	51.96±13.42	45.64±20.32	20.84±4.78	17.55±2.66
	Monsoon	Range (min, max)	(9.30, 32.59)	(11.20, 42.65)	(21.70, 67.55)	(40.40, 73.49)	(2.80, 17.03)	(14.00, 25.3)
	Premonsoon	Mean±std dev	24.20±10.27	32.11±12.73	44.05±19.18	58.49±13.78	11.11±5.53	18.15±4.74
S7	Monsoon	Range (min, max)	(15.20, 40.01)	(17.40, 32.6)	(55.92, 122.8)	(49.02, 67.5)	(3.10, 14.76)	(7.50, 15.19)
	Premonsoon	Mean±std dev	27.61±17.54	25.00±10.75	89.36±47.29	58.26±13.07	(9.33±8.24)	11.35±5.44
	Post monsoon	Range (min, max)	(0.24, 32)	(0.43, 44)	(27.72, 59.44)	(33.59, 74)	(18.40, 23.33)	(15.20, 25.1)
	Premonsoon	Mean±std dev	21.64±14.48	29.02±19.80	(49.59±14.78)	57.05±17.11	21.67±2.28	20.77±4.41
S8	Monsoon	Range (min, max)	(14.69, 29.1)	(6.60, 127.2)	(19.13, 56.3)	(47.20, 62.9)	(1.20, 17.6)	(11.44, 22.7)
	Premonsoon	Mean±std dev	21.60±6.94	40.06±49.55	37.87±16.46	52.07±6.50	9.16±7.60	18.25±4.96
	Post monsoon	Range (min, max)	(14.20, 17.8)	(16.80, 19.19)	(27.93, 53.2)	(27.38, 32.6)	(3.50, 7.26)	(7.10, 10.7)
	Premonsoon	Mean± std dev	16.00±2.55	18.00±1.69	(40.57±17.87)	29.99±3.69	5.38±2.66	8.90±2.55
S9	Monsoon	Range (min, max)	(19.04, 45.6)	(22.79, 41.6)	(43.40, 68)	(22.07, 68)	(12.00, 21)	54.94±8.57
	Premonsoon	Range (min, max)	29.48±14.16	32.46±9.16	53.73±12.76	45.09±22.97	16.94±4.56	(47.65, 99.6)
	Monsoon	Mean±std dev	(12.90, 29.08)	(14.40, 23.48)	(24.60, 41.06)	(35.66, 51.6)	(2.00, 12.96)	18.16±1.85
	Post monsoon	Range (min, max)	(12.90, 29.08)	(14.40, 23.48)	(24.60, 41.06)	(35.66, 51.6)	(2.00, 12.96)	74.42±26.01
S10	Monsoon	Range (min, max)	(15.10, 23.92)	(14.30, 21.42)	(36.98, 65.6)	(29.32, 72.8)	(6.20, 10.88)	(7.10, 11.6)
	Premonsoon	Mean±std dev	(12.90, 29.08)	(14.40, 23.48)	(24.60, 41.06)	(35.66, 51.6)	(2.00, 12.96)	(45.80, 76)

Table 2 (continued)

Location	Season	Statistics	Cu		Ni		Co		Zn	
			Bulk	-63 µm	Bulk	-63 µm	Bulk	-63 µm	Bulk	-63 µm
Post monsoon	Mean±Std dev	Range (min, max)	18.84±4.56	18.54±3.75	54.23±15.19	53.71±22.22	8.26±2.39	9.02±2.32	60.26±15.14	
Post monsoon	Mean±std dev	Mean±std dev	369.50±61.52	7.55±2.05	30.60±31.68	92.05±41.08	235.50±120.92	0.10±0.00	0.75±0.21	
Location	Zn	Pb	Cr		Cd		Cd		Cd	
			Bulk	-63 µm	Bulk	-63 µm	Bulk	-63 µm	Bulk	-63 µm
S1	(63.8, 150)	(3.5, 45.1)	(10.41, 38)	(210, 429.1)	(212.6, 2,200)	(0.53, 3.9)	(0.06, 4.2)			
	104.38±35.33	21.36±18.04	30.15±13.20	282.51±99.38	799.75±941.13	1.88±1.78	2.07±2.24			
	(326, 413)	(6.1, 9)	(8.2, 53)	(63, 121.1)	(150, 321)	(0.1, 0.1)	(0.6, 0.9)			
	369.50±61.52	7.55±2.05	30.60±31.68	92.05±41.08	235.50±120.92	0.10±0.00	0.75±0.21			
S2	(54.6, 164.38)	(0.8, 29.1)	(15.6, 50.59)	(99.2, 274.4)	(131.4, 2,320)	(0.5, 2.3)	(0.2, 2.7)			
	102.17±50.78	12.57±11.99	33.45±14.29	162.05±79.56	749.64±1,050.22	1.14±0.83	1.22±1.17			
	(30.68, 415)	(8.2, 36.34)	(8, 23.31)	(66.5, 151.85)	(78.07, 421)	(0.26, 0.3)	(0.42, 0.9)			
	248.93±197.40	18.51±15.50	17.44±8.25	105.12±43.25	230.02±174.76	0.29±0.02	0.64±0.24			
	(81.08, 131.8)	(22, 23.83)	(18.6, 22.4)	(77.4, 233.59)	(125, 222.85)	(0.299, 1)	(0.399, 1.2)			
	99.36±28.17	14.88±11.29	20.13±2.01	130.73±89.10	162.35±52.87	0.70±0.36	0.87±0.42			
	(60.82, 349.1)	(7.5, 36.9)	(10.76, 41.2)	(119.8, 341.7)	(121.2, 2,690)	(0.2, 2.78)	(0.48, 3.1)			
	127.84±123.88	17.18±11.52	23.20±11.60	204.24±100.68	718.06±1,110.39	1.08±1.10	1.45±1.01			
	(72.63, 226)	(3.4, 22.91)	(13.1, 33.01)	(78.9, 169.1)	(129, 159.1)	(0.3, 0.359)	(0.33, 0.6)			
	134.94±80.62	12.44±9.83	20.37±10.99	126.37±45.29	139.96±16.63	0.32±0.03	0.44±0.14			
	(46.32, 93.8)	(4.07, 28.12)	(11.43, 22.76)	(103.2, 239.4)	(117.2, 200.19)	(0.099, 1)	(0.09, 1.2)			
	68.57±20.01	13.35±11.42	17.05±4.64	170.30±74.71	160.75±41.87	0.58±0.48	0.70±0.50			
S4	(61.2, 240.25)	(1.11, 32.8)	(6.5, 42)	(101.8, 382)	(90.2, 2,850)	(0.1, 3.8)	(0.39, 2.8)			
	120.94±65.55	20.71±11.87	26.08±15.02	217.17±127.20	638.56±1,086.60	1.30±1.70	1.29±1.06			
	(58.22, 146.9)	(3.70, 20.32)	(6.10, 18.85)	(49.80, 142.87)	(111.90, 181)	(0.20, 0.579)	(0.40, 0.5)			
	100.44±44.49	12.67±8.39	12.32±6.38	108.26±50.91	136.26±38.80	0.36±0.20	0.44±0.06			
	(41.00, 104.4)	(2.88, 36.58)	(8.40, 30.73)	(101.80, 299.79)	(94.00, 261.53)	(0.13, 1)	(0.09, 1)			
	79.80±28.15	17.17±14.61	21.30±9.58	176.05±90.76	184.31±69.11	0.61±0.38	0.57±0.50			
	(39.80, 399.84)	(16.70, 33.5)	(13.80, 41.36)	(59.00, 276.1)	(83.80, 5,890)	(0.04, 11)	(1.00, 4.3)			
	134.62±149.48	23.55±8.61	25.96±11.67	175.40±94.34	1,327.8±2,553.31	2.95±4.62	1.84±1.39			
	(66.70, 351.9)	(14.00, 22.15)	(19.00, 24.78)	(134.43, 154.9)	(115.19, 176.9)	(0.39, 0.6)	(0.36, 0.4)			
	209.30±201.67	18.08±5.76	21.89±4.09	144.67±14.47	146.05±43.64	0.49±0.15	0.38±0.03			

Table 2 (continued)

Location	Zn	Pb		Cr		Cd	
		-63 μm	Bulk	-63 μm	Bulk	-63 μm	Bulk
-63 μm							
S6	(70.03, 109.6)	(9.00, 23.02)	(1.89, 25.82)	(72.20, 246.8)	(94.00, 300.1)	(0.09, 1.2)	(0.16, 0.8)
	94.35±17.00	15.70±5.89	15.93±10.39	156.95±87.29	175.60±95.79	0.72±0.49	0.59±0.30
	(51.00, 234.84)	(8.70, 34.86)	(5.80, 95.86)	(35.21, 394.3)	(102.68, 760)	(0.16, 5.3)	(0.04, 2.5)
	138.79±77.92	19.36±10.46	37.52±36.34	154.64±146.05	317.09±277.42	1.79±2.42	1.25±1.23
	(47.21, 172)	(12.00, 18.86)	(16.00, 21.79)	(96.11, 151)	(81.72, 125)	(0.51, 0.7)	(0.40, 0.479)
	109.61±88.24	15.43±4.85	18.90±4.09	123.56±38.81	103.36±30.60	0.61±0.13	0.44±0.06
	(55.98, 105.4)	(11.40, 24.6)	(9.80, 30.48)	(83.80, 178.6)	(76.00, 176.6)	(0.03, 1)	(0.14, 1)
	81.06±24.72	18.67±6.70	21.03±10.45	141.20±50.47	143.07±58.08	0.68±0.56	0.65±0.45
S7							
	(59.38, 154)	(13.00, 19.59)	(12.00, 25.16)	(106.00, 111.87)	(105.30, 108)	(0.42, 0.6)	(0.48, 0.5)
S8	(59.38, 154)	(13.00, 19.59)	(12.00, 25.16)	(106.00, 111.87)	(105.30, 108)	(0.42, 0.6)	(0.48, 0.5)
S8	(50.46, 215.8)	(7.20, 20.27)	(14.00, 22.92)	(69.90, 138.9)	(92.65, 118.9)	(0.10, 0.319)	(0.40, 0.6)
	151.69±88.70	14.16±6.58	18.34±4.46	108.47±55.21	105.38±13.14	0.24±0.12	0.48±0.11

Table 3 (continued)

Loc	Season	Statistics	Fe		Mn		Ca	
			Bulk	-63 µm	Bulk	-63 µm	Bulk	-63 µm
Monsoon	Range (min, max)	(12,690.0, 49,780.0)	(30,060.0, 40,860.0)	(400.00, 740.00)	(400.00, 730.00)	(1,920.00, 4,600.00)	(3,120.00, 4,600.00)	
	Mean±std dev	34,623.33±19,451.46	35,173.33±5,422.78	523.33±188.24	600.00±175.7	3,136.67±1,356.92	3,946.67±755.07	
Post monsoon	Range (min, max)	(990.00, 8,610.00)	(7,400.00, 7,610.00)	(5,010.00, 13,130.0)	(5,200.00, 8,190.00)	(15,400.0, 15,910.0)	(9,110.00, 15,110.0)	
	Mean±std dev	4,800.00±5,388.15	7,505.00±148.49	9,070.00±5,741.71	6,695.00±2,114.25	15,655.00±360.62	12,110.00±4,242.64	
Loc	Mg	Na		K		Ca		
		Bulk	-63 µm	Bulk	-63 µm	Bulk	-63 µm	
S1	(9,280.00, 18,200.0)	(6,200.00, 20,840.0)	(11,900.0, 29,600.0)	(4,500.00, 20,100.0)	(5,600.00, 22,340.0)	(4,500.00, 21,690.0)		
	13,890.00±4,329.45	13,245.00±6,752.90	18,902.50±7,933.94	10,987.50±7,026.19	13,937.50±8,406.31	11,720.00±7,388.20		
	(990.00, 8,610.00)	(7,400.00, 7,610.00)	(5,010.00, 13,130.0)	(5,200.00, 8,190.00)	(15,400.0, 15,910.0)	(9,110.00, 15,110.0)		
	4,800.00±5,388.15	7,505.00±148.49	9,070.00±5,741.71	6,695.00±2,114.25	15,655.00±360.62	12,110.00±4,242.64		
S2	(5,640.00, 15,600.0)	Na		K		Ca		
		Bulk	-63 µm	Bulk	-63 µm	Bulk	-63 µm	
	(5,800.00, 17,150.0)	(12,300.0, 36,500.0)	(2,600.00, 12,560.0)	(6,800.00, 23,540.0)	(7,200.00, 21,890.0)			
	10,520.00±5,155.89	12,980.00±5,280.20	19,370.00±11,465.31	8,442.50±4,249.65	14,997.50±7,639.68	11,970.00±6,734.45		
	(2,690.00, 15,700.0)	(6,230.00, 7,000.00)	(1,100.00, 6,850.00)	(800.00, 7,690.00)	(1,300.00, 20,100.0)	(1,100.00, 12,100.0)		
	7,570.00±7,087.80	6,510.00±425.79	3,720.00±2,908.73	3,893.33±3,498.43	11,153.33±9,432.74	7,963.33±5,985.49		
	(14,430.0, 20,300.0)	(12,620.0, 14,260.0)	(10,260.0, 20,450.0)	(10,440.0, 18,930.0)	(14,320.0, 21,640.0)	(10,980.0, 24,800.0)		
	17,810.00±3,034.52	13,226.67±899.41	15,030.00±5,126.00	14,143.33±4,347.44	18,346.67±3,714.69	16,886.67±7,125.18		
	(8,890, 20,770.0)	(9,600, 26,740.0)	(9,900.00, 32,400.0)	(7,430.00, 13,860.0)	(8,800.00, 23,260.0)	(6,400.00, 23,080.0)		
	11,608.00±7,736.42	12,920.00±9,817.00	18,558.00±8,457.98	9,496.00±2,560.01	14,742.00±6,525.23	12,632.00±6,891.63		
	(6,680.00, 14,300.0)	(7,10.00, 17,800.0)	(1,200.00, 30,900.0)	(1,000.00, 9,810.00)	(1,400.00, 30,010.0)	(1,400.00, 13,780.0)		
	9,490.00±4,185.22	10,896.67±5,988.41	13,136.67±15,683.91	6,706.67±4,948.44	14,716.67±14,407.06	9,130.00±6,740.24		
	(9,100.00, 14,330.0)	(3,930.00, 19,600.0)	(14,520.0, 24,900.0)	(9,860.00, 19,600.0)	(16,300.0, 19,800.0)	(12,340.0, 24,560.0)		
	12,202.50±2,210.65	12,492.50±6,547.03	18,622.50±4,612.28	13,570.00±4,411.88	18,052.50±1,487.18	16,535.00±5,562.31		
	(10,300.0, 24,590.0)	(8,200.0, 28,750.0)	(5,700.0, 22,950.0)	(2,800.00, 13,180.0)	(7,200.0, 23,700.0)	(5,310.0, 24,560.0)		
	14,107.50±6,995.85	17,314.00±8,404.86	16,328.33±6,199.94	8,750.00±3,865.34	13,078.33±6,173.86	14,065.00±8,113.38		
	(7,490.00, 13,500.0)	(6,490.00, 16,600.0)	(1,500.00, 38,700.0)	(1,000.00, 9,310.0)	(1,300.00, 29,610.0)	(1,500.00, 14,630.0)		
	9,733.33±3,281.83	10,293.33±5,500.28	16,116.67±19,838.37	5,326.67±4,165.63	14,646.67±14,224.07	8,340.00±6,582.26		
	(13,410.0, 20,540.0)	(5,190.00, 20,740.0)	(7,650.00, 18,580.0)	(7,860.00, 18,390.0)	(14,530.0, 22,140.0)	(14,560.0, 24,580.0)		
	17,197.50±2,944.13	15,480.00±7,203.32	14,627.50±4,922.46	12,567.50±4,513.83	18,722.50±3,483.37	17,675.00±4,699.54		
	(9,800.00, 21,000.0)	(6,900.00, 23,090.0)	(6,600.00, 28,060.0)	(4,200.00, 14,510.0)	(7,010.00, 21,300.0)	(7,200.00, 23,610.0)		
	13,655.00±5,050.42	17,135.00±7,137.57	15,826.00±9,257.74	9,544.00±4,291.59	12,468.00±6,753.77	12,912.00±7,412.31		
	(8,790.00, 13,600.0)	(9,490.00, 17,600.0)	(1,400.00, 51,700.0)	(1,000.00, 9,150.00)	(1,000.00, 12,680.0)	(1,600.00, 14,130.0)		

Table 3 (continued)

Loc	Mg	Na		K	
		Bulk	-63 μm	Bulk	-63 μm
S6	11,195.00±3,401.18 (11,860.0, 22,480.0)	13,545.00±5,734.64 (4,570.00, 18,040.0)	26,550.00±35,567.47 (9,550.00, 22,980.0)	5,075.00±5,762.92 (2,340.00, 12,340.0)	6,840.00±8,259.01 (10,890.0, 22,340.0)
	17,445.00±4,735.49 (5,760.00, 18,080.0)	13,927.50±6,376.63 (6,400.00, 18,020.0)	15,777.50±5,719.17 (9,500.00, 23,680.0)	9,362.50±4,759.69 (5,500.00, 14,200.0)	15,375.00±5,106.13 (6,300.00, 25,060.0)
	11,602.50±5,139.61 (8,090.00, 16,100.0)	13,417.50±5,259.29 (6,090.00, 16,100.0)	15,624.00±6,658.44 (1,200.00, 49,200.0)	9,716.00±3,896.44 (1,100.00, 8,850.00)	12,746.00±8,120.37 (1,400.00, 13,250.0)
	12,095.00±5,663.93 (18,060.0, 21,040.0)	11,095.00±7,078.14 (4,190.00, 22,180.0)	25,200.00±33,941.13 (11,970.0, 27,980.0)	4,975.00±5,480.08 (12,160.0, 14,340.0)	7,325.00±8,379.22 (13,360.0, 24,960.0)
	19,406.67±1,510.54	16,063.33±10,284.18	19,116.67±8,141.88	13,326.57±1,098.06	18,266.67±6,002.84
	S7				
	(8,090.00, 15,600.0) 11,845.00±5,310.37	(8,290.00, 16,100.0) 12,195.00±5,522.50	(1,300.00, 35,000.0) 18,150.00±23,829.50	(1,000.00, 8,660.00) 4,830.00±5,416.44	(1,400.00, 14,250.0) 7,825.00±9,086.32
	S8				
	(4,530.00, 15,100.0) 9,706.67±5,288.33	(7,310.00, 13,300.0) 9,600.00±3,234.36	(1,300.00, 50,100.0) 29,000.00±25,060.53	(1,100.00, 8,770.00) 5,826.67±4,134.30	(1,600.00, 15,300.0) 9,146.67±6,955.47

the studied pollutants since this method tends to reduce the outliers, which might bias the reported results. Similarly, the PLI is broadly divided into three significant categories for comparative assessment of pollution level in the study area viz., where a value of $\text{PLI} < 1$ denotes perfection, $\text{PLI}=1$ presents that only baseline levels of pollutants, and $\text{PLI} > 1$ would indicate deterioration of site quality (Tomlinson et al. 1980).

Index of geoaccumulation

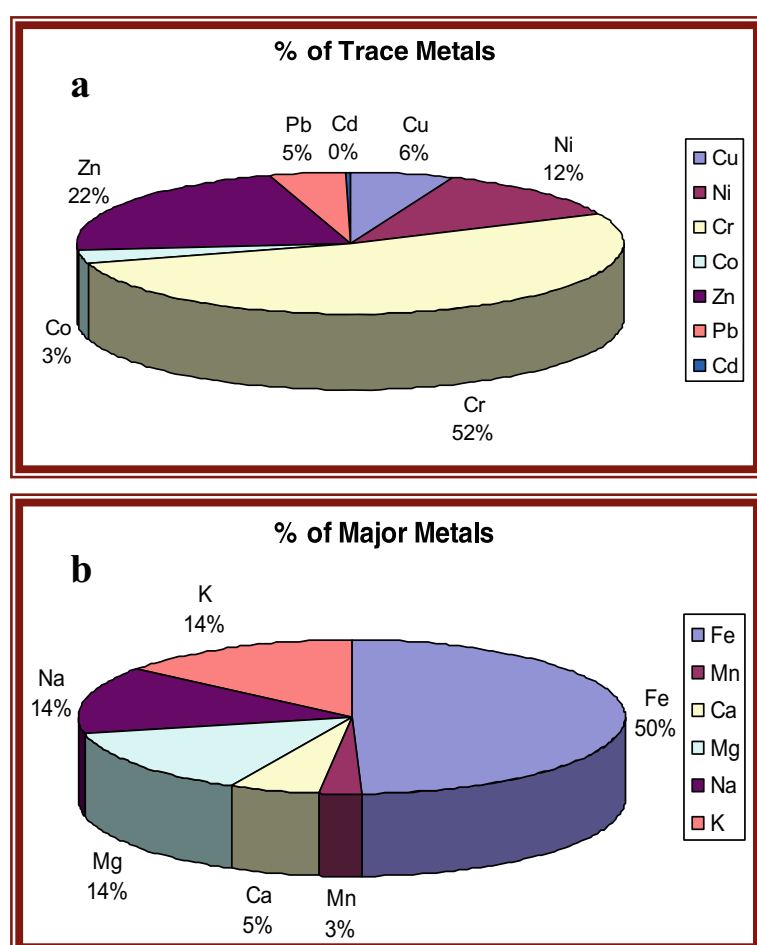
Geoaccumulation index (I_{geo}) was used to assess heavy metal accumulation in sediments as introduced by Muller (1969) to measure the degree of metal pollution in aquatic sediments studies. This index allows assessing the degree of contamination in the polluted sediment by comparing present concentrations with pre-industrial levels. I_{geo} was calculated using the method proposed by Muller

(1969), termed as the I_{geo} . The formula used for the calculation of I_{geo} is as follows:

$$I_{\text{geo}} = \log_2 [C_n \text{Sample} / (1.5 \times C_n \text{Background})]$$

where $C_n \text{Sample}$ is the measured content of n th element, and $C_n \text{Background}$ is the element content in an average shale (Turekian and Wedepohl 1961). The concentrations of geochemical background are multiplied each time by the constant 1.5 in order to allow content fluctuations of a given substance in the environment as well as the very small anthropogenic influences. The I_{geo} was originally defined by Muller (1969) for a quantitative measure of the metal pollution in aquatic sediments (Ridgway and Shimmield 2002). Muller (1969) has distinguished six classes of the geoaccumulation index as shown in Table 1. Class 6 is an open class and comprises all values of the geoaccumulation index higher than 5.

Fig. 2 Percentages of contribution of **a** trace metals and **b** major metals in Dhamra marine sediments



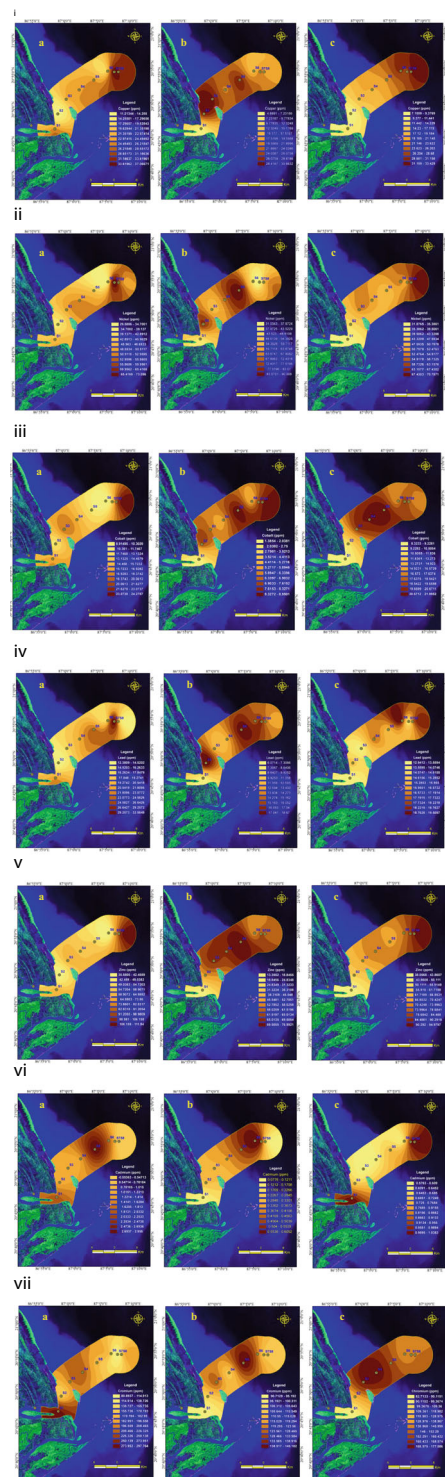


Fig. 3 Marine sediment trace metals interpolation maps depicting the distribution of each metal contribution for **a** premonsoon, **b** monsoon, and **c** post monsoon superimposed upon pan-sharpened Landsat ETM+ imagery

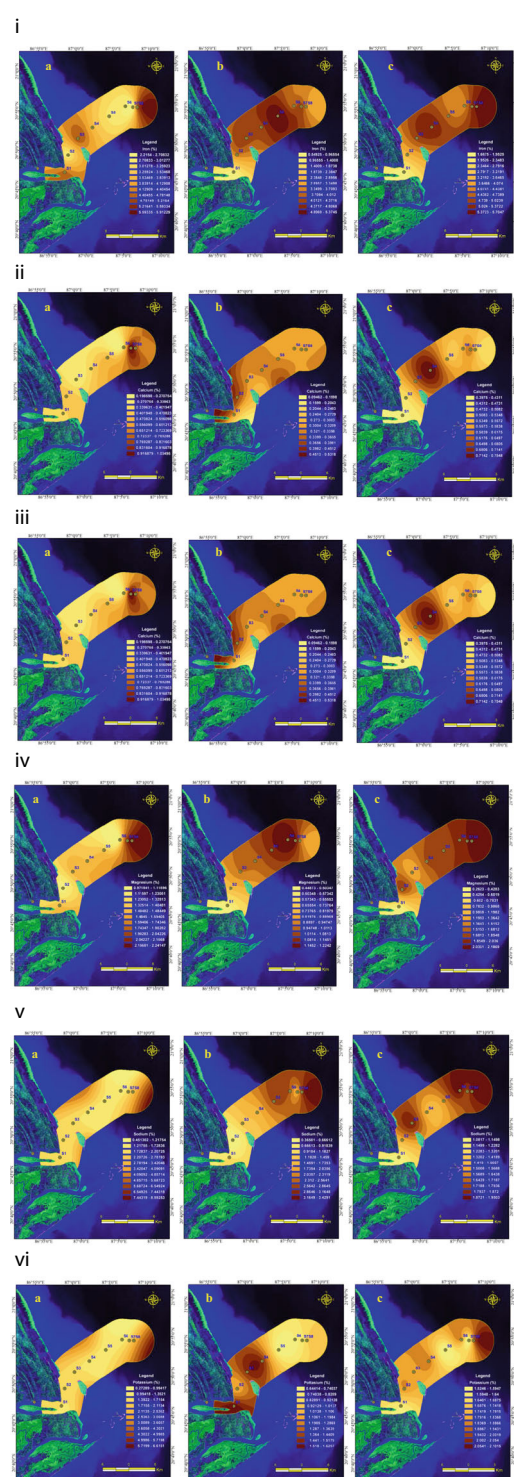


Fig. 4 Marine sediment major metals interpolation maps depicting the distribution of each metal contribution for **a** premonsoon, **b** monsoon, and **c** post monsoon superimposed upon pan-sharpened Landsat ETM+ imagery

Geospatial analysis

This approach has been applied employing various statistical and informational techniques to geographically based data of the study area using softwares viz., ERDAS Imagine, ArcGIS (ESRI, USA), SPSS, etc.

Geostatistical approach

The distribution patterns of seven trace metals and six major metals, whose concentrations were measured using AAS, were depicted through the interpolation of elemental concentrations in bulk as well as in $-63\text{ }\mu\text{m}$ by using geostatistical techniques i.e., cokriging in ArcGIS platform in the buffer area of 5 km along the dredging channel. The impact of the dredging channel on the Bay is thus assessed by developing a pollution load index map for the study area considering all the elements found in sediment samples using raster calculator in GIS adapting PLI developed by Tomlinson et al..

In order to facilitate further interpretation of local spatial variations, continuous spatial distributions of all discriminant variables (Cu, Ni, Co, Pb, Zn, Cr, Cd, Fe, Mn, Ca, Mg, Na, K) were generated based on kriging in GIS (Wang 2006). Major and trace metal concentrations in marine sediment database were converted into shape file formats in GIS. Spatial coordinates of the sampling locations were fixed using GPS model Trimble Juno

with minimum 3-m accuracy. For each season, samples were being collected by navigating to the fixed locations. In the present study, the spatial analysis is being carried out within 5 km buffer region of the channel owing to port activity. The coordinate system WGS 1984 UTM Zone 45 N was used for generating the metal concentration layers in sediments. Though the sample size of 8 is few to get an accurate depiction, an attempt has been made to get the spatial pattern of the study area for various pollution indices.

Principal component analysis of metal concentrations

Generally, principal component analysis (PCA) is a common multivariate statistical technique being widely used to identify pollution sources and to apportion geogenic versus anthropogenic contamination (Atteia et al. 1994; Tao 1995; Facchinelli et al. 2001; Zhou et al. 2007). PCA or factor analysis (FA) is a robust technique which converts the variables (metal concentrations) that are inter-correlated (Wiechula et al. 2003). The first factor explains the most variance; the second factor the next most and so on. The dimensionality can be reduced to a few factors commonly two or three retaining most of the overall variance. Factors can also be rotated in such a way that each factor explains a different subset of correlated variables. The samples with similar analytical compositions are aggregated

Fig. 5 Shepard sand-silt-clay ternary plot (texture) mean value near Dhamra coast

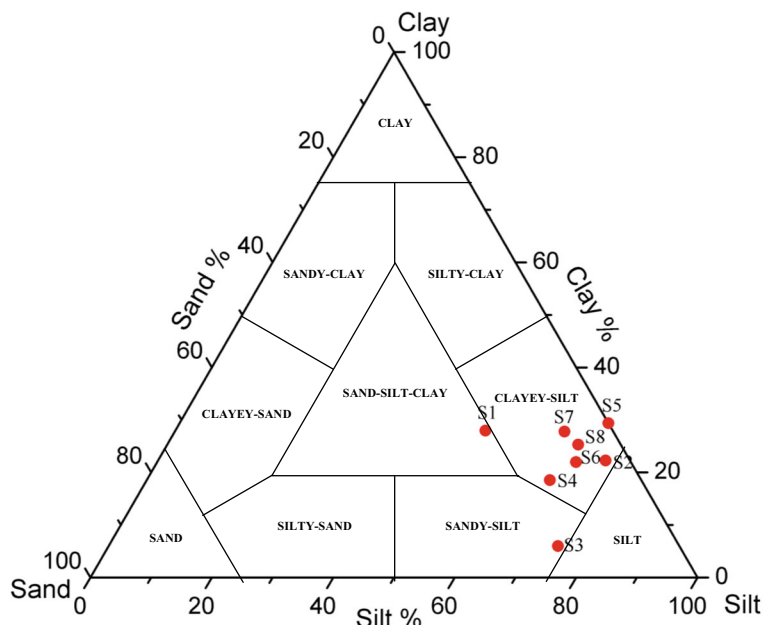


Table 4 Statistics of organic carbon (%) in marine sediment near Dhamra estuary

Location	Season	Statistics	Organic carbon	
			Bulk	-63 µm
S1	Premonsoon	Range (min, max)	0.20–1.84	1.05–1.82
		Mean±std dev	1.28±0.74	1.38±0.35
		Monsoon	Range (min, max)	0.20–0.73
	Post monsoon	Range (min, max)	0.46±0.38	1.18±0.03
		Mean±std dev	0.22–1.07	0.41–1.31
		Mean±std dev	0.64±0.60	0.86±0.64
S2	Premonsoon	Range (min, max)	0.02–1.63	0.29–1.23
		Mean±std dev	0.78±0.78	0.62±0.44
		Monsoon	Range (min, max)	0.22–0.80
	Post monsoon	Range (min, max)	0.47±0.29	0.81–1.57
		Mean±std dev	0.05–1.15	1.28±0.41
		Mean±std dev	0.52±0.47	0.42–2.02
S3	Premonsoon	Range (min, max)	0.19–2.47	1.01–1.88
		Mean±std dev	1.46±0.91	1.42±0.38
		Monsoon	Range (min, max)	1.21–1.94
	Post monsoon	Range (min, max)	1.64±0.38	1.01–1.65
		Mean±std dev	0.73–1.61	1.42±0.36
		Mean±std dev	1.11±0.44	0.65–1.83
S4	Premonsoon	Range (min, max)	0.45–4.97	1.27±0.42
		Mean±std dev	1.80±1.63	0.25–1.98
		Monsoon	Range (min, max)	1.01–1.50
	Post monsoon	Range (min, max)	1.27±0.24	0.84–1.76
		Mean±std dev	0.68–1.91	1.17±0.51
		Mean±std dev	1.37±0.51	0.73–1.50
S5	Premonsoon	Range (min, max)	0.16–2.56	1.14±0.36
		Mean±std dev	1.05±1.02	0.61–1.39
		Monsoon	Range (min, max)	1.71–2.19
	Post monsoon	Range (min, max)	1.95±0.34	1.35–1.57
		Mean±std dev	0.05–1.58	1.46±0.16
		Mean±std dev	0.99±0.59	0.52–2.16
S6	Premonsoon	Range (min, max)	0.19–1.74	0.99±0.59
		Mean±std dev	1.10±0.69	0.63–1.35
		Monsoon	Range (min, max)	0.59–2.25
	Post monsoon	Range (min, max)	1.42±1.17	0.42–1.51
		Mean±std dev	0.64–2.04	0.96±0.77
		Mean±std dev	1.24±0.59	0.48–2.15
S7	Premonsoon	Range (min, max)	NA	1.23±0.59
		Mean±std dev	NA	NA
		Monsoon	Range (min, max)	1.16–1.58
	Post monsoon	Range (min, max)	1.37±0.30	0.01–0.93
		Mean±std dev	NA	0.47±0.65
		Mean±std dev	NA	NA
S8	Premonsoon	Range (min, max)	NA	NA
		Mean±std dev	NA	NA
		Monsoon	Range (min, max)	1.45–1.98
	Post monsoon	Range (min, max)	1.73±0.27	0.86–1.58
		Mean±std dev	NA	1.23±0.36
		Mean±std dev	NA	NA

min Minimum, max Maximum,
std dev Standard Deviation, NA
Not Available

Table 5 Varimax-rotated principal component analysis and source of metal enrichment in marine sediments

Variables	PC1	PC2	PC3
Ca	-0.447	0.625	-0.286
Cd	0.924	0.159	-9.44E-02
Co	0.614	0.698	0.169
Cr	0.896	3.92E-02	-5.43E-02
Cu	0.781	0.173	-0.137
Fe	0.286	0.25	-2.74E-02
K	-2.43E-02	0.881	-5.75E-02
Mg	0.513	0.582	0.41
Mn	0.786	-4.87E-02	4.80E-02
Na	0.202	0.924	-6.34E-02
Ni	0.403	-0.191	0.107
OC	-5.51E-03	3.40E-02	0.341
Pb	0.717	-2.90E-02	-0.42
Zn	-5.07E-02	-0.575	-0.518
Eigenvalue	7.391	6.592	4.637
Percentage of variance	26.395	23.541	16.560

closer than those with more dissimilar compositions. The similarities among samples can then be used to elucidate potential sources (Einax et al. 1997). A varimax rotation is employed to aid in interpretability of the low-variance principal components. This makes closer to finding unique metal concentration related to outcome but reintroduces correlation requiring analysis of the overlap of information contained in such modes. Varimax rotation perturbs the eigenvectors so as to maximize the variance within each vector. As a result

in each vector, the number of variables with immediate loading is decreased and the number with either very large or very small loading is increased (Satapathy et al. 2009).

Correlation of metal enrichment in marine sediments

The correlation matrix used in this study provides an important tool for better understanding of the complex dynamics of pollutants in riverine and marine system. The analysis was performed to determine the significant relationship among various metals and organic carbon and its enrichment in marine sediments. The data has correlated with the mean values of geochemical data of metals and organic carbon. The values in the matrix represent the correlation coefficients ranging from negative correlation to positive correlation (-1 to +1).

Results and discussion

Major and trace metals in marine sediments

The derived statistics of major and trace metal concentration database for all the seasons is represented in Tables 2 and 3. The contribution of individual metal is calculated by calculating the percentage of average concentration of each metal to the total average concentration of all the metals in the sample in all throughout the seasons separately for trace and major metals

Table 6 Cross-correlation matrix of major/trace metals in marine sediments

	Ca	Cd	Co	Cr	Cu	Fe	K	Mg	Mn	Na	Ni	OC	Pb	Zn
Ca	1.000	NA	NA	NA	NA	NA	NA	NA	NA	NA	NA	NA	NA	NA
Cd	-0.396	1.000	NA	NA	NA	NA	NA	NA	NA	NA	NA	NA	NA	NA
Co	0.004	0.702	1.000	NA	NA	NA	NA	NA	NA	NA	NA	NA	NA	NA
Cr	-0.358	0.897	0.540	1.000	NA	NA	NA	NA	NA	NA	NA	NA	NA	NA
Cu	-0.155	0.734	0.652	0.619	1.000	NA	NA	NA	NA	NA	NA	NA	NA	NA
Fe	0.050	0.258	0.309	0.078	0.550	1.000	NA	NA	NA	NA	NA	NA	NA	NA
K	0.574	0.108	0.568	0.029	0.082	0.197	1.000	NA	NA	NA	NA	NA	NA	NA
Mg	0.102	0.422	0.747	0.455	0.411	0.253	0.495	1.000	NA	NA	NA	NA	NA	NA
Mn	-0.271	0.607	0.383	0.604	0.486	0.176	-0.012	0.452	1.000	NA	NA	NA	NA	NA
Na	0.484	0.366	0.758	0.183	0.261	0.299	0.835	0.595	0.137	1.000	NA	NA	NA	NA
Ni	-0.169	0.299	0.122	0.328	0.483	0.144	-0.095	0.063	0.265	-0.147	1.000	NA	NA	NA
OC	0.017	0.010	0.063	-0.053	0.075	0.238	0.125	-0.075	0.027	0.079	0.470	1.000	NA	NA
Pb	-0.264	0.645	0.389	0.519	0.731	0.423	-0.042	0.212	0.488	0.179	0.212	-0.194	1.000	NA
Zn	-0.139	-0.103	-0.561	-0.061	-0.041	0.099	-0.366	-0.606	-0.041	-0.498	0.307	0.207	0.243	1.000

NA Not Available

Table 7 (continued)

Location	Season	Period	Cu	Ni	Co	Zn			Pb	Cr	Cd
						Bulk	-63 µm	Bulk			
Monsoon	Post monsoon	Mar 11	0.84	1.06	1.29	1.34	0.94	0.99	3.21	0.94	2.32
		Jul. 09	0.31	0.28	1.83	0.71	0.13	0.41	1.71	0.77	1.62
		Aug. 09	0.52	0.97	0.81	0.84	0.09	0.37	0.91	1.13	0.21
	Premonsoon	Aug. 10	0.77	0.73	0.76	0.76	0.81	0.78	0.72	0.69	1.15
		Nov. 09	0.29	0.47	0.44	0.43	0.48	0.57	0.45	0.66	0.32
		Dec. 09	0.73	0.77	0.80	0.72	0.97	0.96	0.83	0.96	0.85
		Oct. 10	0.51	0.40	0.64	0.31	1.51	1.15	0.65	0.53	2.23
S5	Premonsoon	Dec. 10	0.01	0.00	0.94	0.95	1.32	0.78	0.94	0.83	0.15
		Mar. 09	NA	0.52	0.66	1.23	0.31	1.53	0.43	0.87	3.48
		May 09	0.30	0.96	0.58	1.12	0.79	1.90	0.63	0.94	1.19
		Mar. 10	0.54	0.66	0.69	0.67	0.68	0.69	0.74	0.75	0.72
		Apr. 10	1.42	2.23	1.71	2.53	1.27	1.94	1.27	2.20	3.92
		Mar. 11	2.12	2.77	2.91	3.16	2.62	3.18	2.29	12.32	2.65
		Monsoon	Jul. 09	0.28	0.32	1.49	0.82	0.13	0.33	0.69	3.05
Post monsoon	Premonsoon	Aug. 10	0.84	0.68	0.77	0.68	0.73	0.75	0.73	0.66	1.04
		Nov. 09	0.58	0.81	0.72	0.77	0.89	0.73	0.86	0.96	0.41
		Dec. 09	0.68	0.94	0.81	1.04	1.10	0.98	0.86	1.10	0.81
		Oct. 10	0.64	0.77	0.96	0.54	1.34	1.45	0.69	0.81	1.26
		Dec. 10	0.01	0.01	0.52	1.18	1.55	1.55	0.57	1.30	0.87
		Mar. 09	NA	0.95	1.23	2.14	0.19	3.69	0.39	6.60	3.80
		May 09	0.70	0.75	0.90	1.00	0.97	1.29	0.72	0.58	0.47
S6	Premonsoon	Mar. 10	0.70	0.18	0.96	0.87	1.13	0.95	0.93	1.09	0.97
		Apr. 10	NA	NA	NA	NA	NA	NA	NA	NA	NA
		Mar. 11	0.44	0.66	0.38	0.96	0.36	0.82	0.26	1.71	0.86
		Jul. 09	0.33	0.40	0.83	0.51	0.19	0.40	0.68	1.92	0.64
		Aug. 10	0.59	0.63	0.61	0.60	0.57	0.84	0.77	0.74	1.40
		Nov. 09	0.56	0.77	0.77	0.70	0.66	0.92	0.84	0.90	0.60
		Dec. 09	0.87	0.79	0.86	0.86	0.95	0.91	0.90	0.95	1.05
S7	Premonsoon	Oct. 10	0.71	0.85	1.07	0.54	1.57	1.56	0.84	0.99	1.67
		Apr. 10	1.57	1.20	2.05	1.57	1.29	1.09	1.32	1.28	3.09
		Jul. 09	0.32	0.36	0.40	0.84	0.12	0.42	0.73	1.80	0.72
		Aug. 10	0.70	0.57	0.66	0.57	0.74	0.65	0.71	0.68	1.07
		Nov. 09	0.56	0.60	0.71	0.56	0.96	0.75	0.80	0.62	1.11
		Mar. 10	0.75	0.68	0.85	0.77	1.06	0.95	1.01	0.87	0.99
		May 09	0.70	0.57	0.66	0.57	0.74	0.65	0.71	0.68	1.07
S8	Post monsoon	Post monsoon	NA	NA	NA	NA	NA	NA	NA	NA	NA
		Premonsoon	Jul. 09	0.75	0.75	0.77	0.77	0.77	0.77	0.77	0.77

Table 7 (continued)

Location	Season	Period	Cu	Ni		Co		Zn		Pb		Cr		Cd	
				Bulk	-63 µm										
Monsoon	Jul. 09	0.32	0.30	0.91	0.82	0.38	0.35	0.76	2.15	0.71	0.66	1.46	1.25	0.95	1.26
	Aug. 09	1.45	1.64	3.29	3.98	1.21	2.27	1.79	7.39	1.34	3.37	2.89	4.32	1.24	7.44
	Aug. 10	0.61	0.54	0.62	0.49	0.65	0.50	0.71	0.61	1.16	1.31	1.48	1.17	1.21	1.67
Post monsoon	Nov. 09	0.60	0.83	0.81	0.73	0.82	0.96	0.82	1.02	0.73	0.63	1.39	1.29	2.86	2.29

NA Not Available

(Fig. 2a, b). Thus, the percentage of contribution of each trace element in sea sediment is found to be Cr (52 %), Zn (22 %), Ni (12 %), Cu (6 %), Pb (5 %), Co (3 %), and Cd (0.2 %) out of measured trace elements. Similarly, the percentage of contribution of each major element in sea sediment is found to be Fe (50 %), Na (14 %), K (14 %), Mg (14 %), Ca (5 %), and Mn (3 %) out of the measured major elements. The above results indicate that there may be geogenic contamination of metals in sediments through the sediment deposition of Baitarani and Brahmani Rivers passing through many ongoing mining as well as the rock weathering of geological formations reaching Dhamra estuary.

Univariate spatial distribution of elemental concentration

The spatial distributions of elemental concentrations and pollution load index in sediment samples collected from specified sampling locations along the channel near Dhamra estuary are presented as surface maps resulting from kriging interpolation. Besides elemental concentration, other index parameters such as enrichment factor, contamination factor, geoaccumulation index, and pollution load index are equally responsible to conclude that the existing pollution of Cr is attributed to anthropogenic sources (emission from mining activities and its mobility through river), of which few other metals is attributed to geogenic (due to high rock content).

Metal concentrations increase towards eastern part compared to the western part of the study area in premonsoon and post monsoon seasons as depicted from the Figs. 3 and 4 where as it is uniformly distributed throughout the study area during monsoon season. This could be due to the high concentrations of mining, industrial, and urban wastes carried by Brahmani and Baitarani Rivers culminating at Dhamra estuary. The increasing order in concentrations of the metals is observed beyond estuarine region because of the dumping of dredged materials. Finding higher concentration of metals, sparsely located, is particularly due to the enhanced organic carbon content and abundance of clay fractions (Salomons and Forstner 1984).

In the present study, the minimum and maximum concentrations of trace metals are for Cu (0.083 to 127.2 ppm), Ni (17.35 to 122.8 ppm), Co (1.2 to 31.58 ppm), Pb (0.8 to 95.86 ppm), Zn (12.1 to 415 ppm), Cd (0 to 11 ppm), and Cr (35.21 to 5,890 ppm) (Fig. 3). The Cu concentration being higher towards the eastern part

Table 8 (continued)

Location	Season	Period	Mn		Ca		Mg		Na		K	
			Bulk	-63 µm	Bulk	-63 µm	Bulk	-63 µm	Bulk	-63 µm	Bulk	-63 µm
S6	Monsoon	Jul. 09	0.86	0.88	0.07	0.12	0.48	0.52	4.44	0.79	0.39	0.44
		Aug. 10	0.55	0.55	0.20	0.19	0.85	1.11	0.14	0.10	0.04	0.06
	Post monsoon	Nov. 09	0.53	0.53	0.23	0.22	1.23	1.10	1.64	1.18	0.55	0.56
		Dec. 09	0.61	0.68	0.32	0.21	1.43	1.15	2.29	1.22	0.80	0.80
		Oct. 10	1.28	1.38	0.23	0.34	1.13	0.33	1.09	1.20	0.51	0.74
		Dec. 10	0.98	1.43	0.24	0.20	1.00	1.28	1.77	0.31	0.52	0.53
	Premonsoon	Mar. 09	0.62	5.19	0.01	0.01	2.57	1.32	3.05	1.77	0.73	0.38
		May 09	2.11	1.75	0.08	0.04	0.73	0.90	1.17	0.92	0.27	0.35
		Mar. 10	0.94	0.96	0.39	0.43	1.46	1.36	3.00	1.71	1.14	0.79
		Apr. 10	NA	NA	NA	NA	NA	NA	NA	NA	NA	NA
		Mar. 11	98.06	110.56	NA	NA	NA	NA	3.09	1.03	0.46	0.34
S7	Monsoon	Jul. 09	0.98	0.98	0.08	0.16	0.57	0.43	5.42	0.98	0.53	0.56
		Aug. 10	0.70	0.70	0.30	0.30	1.60	1.60	0.19	0.17	0.08	0.08
		Post monsoon	Nov. 09	0.67	0.63	0.32	0.46	1.34	1.53	1.90	1.33	0.65
	Post monsoon	Dec. 09	0.68	0.58	0.22	0.22	1.20	1.27	2.50	1.28	0.80	0.79
		Oct. 10	1.00	2.30	0.32	0.45	2.02	0.47	2.09	2.35	0.84	1.04
		Premonsoon	Apr. 10	1.14	1.26	0.89	0.91	2.71	2.47	3.26	2.74	1.04
S8	Monsoon	Jul. 09	1.02	1.03	0.07	0.16	0.60	0.62	4.06	1.00	0.60	0.61
		Aug. 10	0.64	0.51	0.23	0.22	1.13	1.17	0.15	0.11	0.06	0.06
		Post monsoon	Nov. 09	0.62	0.60	0.26	0.30	1.25	1.22	1.68	1.19	0.53
	Premonsoon	Mar. 10	0.75	0.84	0.36	0.35	1.46	1.57	3.13	1.49	0.92	0.67
		Jul. 09	0.83	0.81	0.08	0.18	0.60	0.52	3.52	0.87	0.55	0.50

NA Not Available

of the study area indicates that the presence of Cu is mainly of the dumping activity which may cause the higher clay fraction and organic content (Harbison 1984). The substantial amount of Ni is observed in the study area due to petroleum-related activity owing to vessel movement (Vazquez and Sharma 2004). In all seasons, Co shows similar distribution pattern as that of Cu and is found to be higher in dumping sites of the marine region than in estuarine region. This is an

indicator of corrosion-resistant paints used for trawlers in the nearby fishing jetty. The average Pb level in Indian River sediment is about 14 mg/kg, which is lower than the world average. Similarly, the average Pb in Indian River particulates is 51 mg/kg which is also lower than the world river particulates of 150 mg/kg (Dekov et al. 1999). In the study area, Pb appears to be higher in the dumping area than estuarine region as marine sediments act as sinks for

Table 9 Contamination factor (CF) (Hakanson 1980) of trace metals in marine sediments

Season	Cu		Ni		Cr		Co		Zn		Pb		Cd	
	Bulk	-63 µm	Bulk	-63 µm	Bulk	-63 µm	Bulk	Bulk	-63 µm	Bulk	-63 µm	Bulk	-63 µm	Bulk
Premonsoon	0.55	0.81	0.94	0.82	1.99	6.65	0.76	1.02	0.62	1.15	1.04	1.50	4.65	4.09
Monsoon	0.47	0.53	0.70	0.76	1.27	1.67	0.34	0.46	0.60	1.88	0.72	0.99	1.22	1.69
Post monsoon	0.46	0.56	0.67	0.62	1.60	1.51	0.89	0.86	0.73	0.81	0.77	0.84	2.62	2.24

Table 10 CF (Hakanson 1980) of major metals in marine sediments

Season	Fe		Mn		Ca		Mg		Na		K	
	Bulk	-63 µm	Bulk	-63 µm	Bulk	-63 µm	Bulk	Bulk	-63 µm	Bulk	-63 µm	Bulk
Premonsoon	0.771	1.275	5.873	8.139	0.231	0.244	0.988	1.083	1.966	1.108	0.568	0.510
Monsoon	0.768	1.012	0.699	0.777	0.147	0.210	0.637	0.680	1.835	0.564	0.410	0.355
Post monsoon	0.927	1.322	0.736	0.828	0.255	0.292	1.085	1.036	1.704	1.306	0.654	0.644

Pb as also seen for Zn. Co, Pb, and Zn depict similar distribution pattern attributing to paint effluents and industrial discharges to the Brahmani River. The maximum concentration of Cd is found beyond estuarine region owing to corrosion-resistant paints which is independent of the accumulation rates of terrigenous detrital input (Calvert and Pedersen 1993). Cr concentration was found to be higher in the off-estuarine region attributing to its source mining wastes discharging into Brahmani River which drains into sea at Dhamra estuary. The Cr and Cu

pollutants in the study area are arising out of industrial wastes, suggesting contribution through sewages (El Nemr et al. 2006).

The range of concentrations of major metals is observed for Fe (7,490 and 169,100 ppm), Mn (20 to 69,188 ppm), Ca (10 to 10,520 ppm), Mg (990 to 28,750 ppm), Na (300 to 51,700 ppm), and K (1,100 to 30,010 ppm) (Fig. 4). In the present study, it is observed that the Fe concentration is somewhat higher than that reported from other Indian estuaries. Concentrations of Fe and Mn are found to be low in near-estuarine region than

Table 11 Pollution load index (PLI) of trace metals in marine sediments

Location	Season	PLI	
		Bulk	-63 µm
S1	Premonsoon	1.234554	1.964565
	Monsoon	0.308307	1.323885
	Post monsoon	0.637664	NA
S2	Premonsoon	0.75167	1.703111
	Monsoon	0.762307	1.087376
	Post monsoon	0.699633	1.09518
S3	Premonsoon	1.069285	1.634436
	Monsoon	0.736275	1.012326
	Post monsoon	0.916642	0.969952
S4	Premonsoon	1.114739	1.79309
	Monsoon	0.713605	0.828888
	Post monsoon	0.990631	1.006557
S5	Premonsoon	1.145991	1.923337
	Monsoon	0.956553	1.049969
	Post monsoon	0.994163	1.087048
S6	Premonsoon	0.908676	1.595058
	Monsoon	0.689634	0.763689
	Post monsoon	1.025636	1.049816
S7	Premonsoon	1.110384	0.878617
	Monsoon	0.716486	0.827416
	Post monsoon	1.065334	1.095686
S8	Premonsoon	1.022135	0.90544
	Monsoon	0.673326	0.884525
	Post monsoon	1.158432	1.18176

NA Not Available

Table 12 PLI of major metals in marine sediments

Location	Season	PLI	
		Bulk	-63 µm
S1	Premonsoon	0.733151	0.603953
	Monsoon	0.330801	0.576304
	Post monsoon	0.416989	NA
S2	Premonsoon	0.630245	0.674588
	Monsoon	0.461583	0.477685
	Post monsoon	0.730364	0.765512
S3	Premonsoon	1.040698	1.048512
	Monsoon	0.594671	0.578159
	Post monsoon	0.810976	0.750334
S4	Premonsoon	0.872948	1.141542
	Monsoon	0.634404	0.533784
	Post monsoon	0.874358	0.785535
S5	Premonsoon	1.062562	1.07011
	Monsoon	0.644528	0.536377
	Post monsoon	0.767091	0.711731
S6	Premonsoon	1.002418	1.082184
	Monsoon	0.600094	0.482393
	Post monsoon	0.805107	0.905843
S7	Premonsoon	0.761159	0.810532
	Monsoon	0.588021	0.490482
	Post monsoon	0.813841	0.899578
S8	Premonsoon	1.02186	1.016033
	Monsoon	0.592095	0.520785
	Post monsoon	0.877487	0.765538

NA Not Available

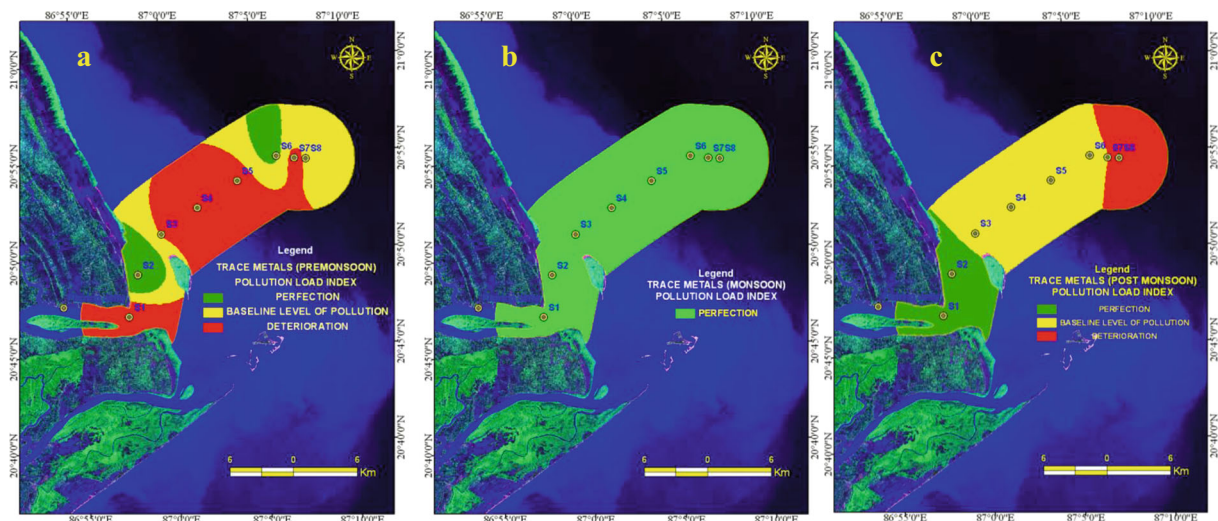


Fig. 6 Pollution load index in marine sediments for trace metals: **a** premonsoon, **b** monsoon, and **c** post monsoon superimposed upon pan-sharpened Landsat ETM+ imagery

offshore region and are attributed towards dumping of the dredged material. Fe and Mn play a vital role in the increase of other metal concentrations. These elements convert to complex hydroxyl compounds which precipitate further to act as good adsorbents (Riley and Chester 1971). On the other hand, Fe and Mn oxides are excellent scavengers for trace metals which lead to co-precipitation of other metals in the water column thus increasing the concentration of other metals in sediments (Tessier et al. 1979). The spatial distribution pattern of other major metals, viz., Ca, Mg, Na, and K, depicts that the

concentration gradually increased beyond the estuarine region towards dumping sites.

The concentration of all metals irrespective of seasons increases towards the offshore region indicating the impact of dredging due to ongoing construction of port and harbor activity. This may be because of continual resuspension of the bottom sediment occurring in Dhamra estuary and dumped in offshore region. The spatial distribution pattern of organic content in sediment and particle size distribution correlates with the concentration of metals in marine sediments. Metal

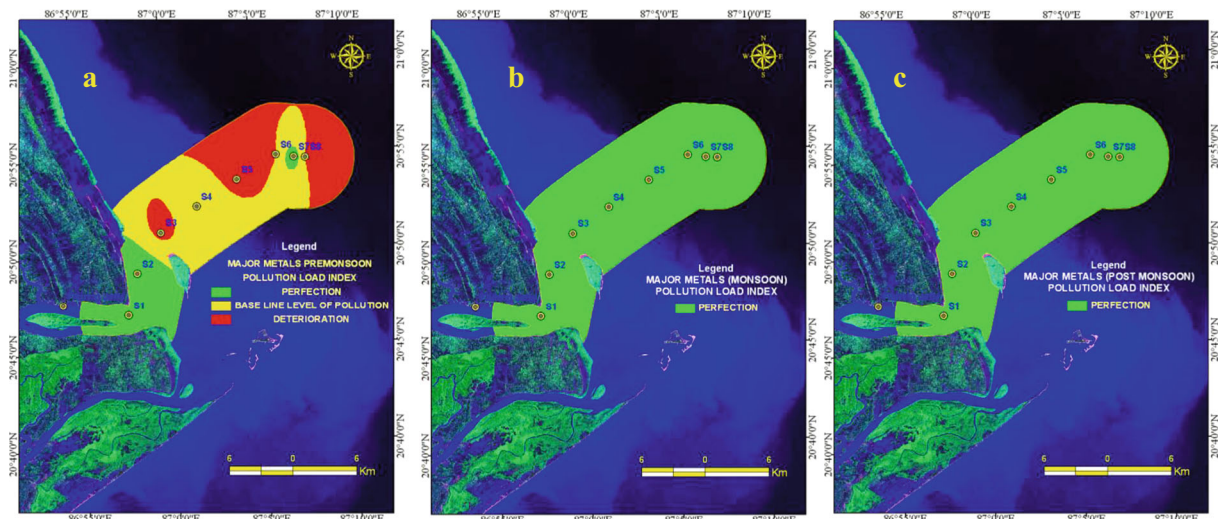


Fig. 7 Pollution load index in marine sediments for major metals: **a** premonsoon, **b** monsoon, and **c** post monsoon superimposed upon pan-sharpened Landsat ETM+ imagery

Table 13 Geoaccumulation index (I_{geo}) of trace metals in marine sediments

Location	Season	Period	Cu	Ni	Co	Zn	Pb	Cr	Cd
			Bulk	-63 µm	Bulk	-63 µm	Bulk	-63 µm	Bulk
			Bulk	-63 µm	Bulk	-63 µm	Bulk	-63 µm	Bulk
S1	Premonsoon	Mar. 09	-1.36	-1.91	-1.22	-0.98	-1.31	-0.53	-1.73
		May 09	-1.01	-0.26	-0.89	-0.51	-0.65	0.06	-1.08
		Mar. 10	-2.40	-0.35	-1.27	-1.03	-1.25	-0.17	-0.91
		Feb. 11	-1.40	-0.43	-1.12	-0.59	-0.27	0.15	-1.30
		Jul. 09	-3.78	-1.02	-1.87	-1.46	-4.57	-3.15	-3.15
		Aug. 09	-2.75	-1.35	-0.78	-0.57	-3.35	-1.48	-2.91
		Dec. 09	-2.78	NA	-1.64	NA	-1.73	NA	-1.83
S2	Post monsoon	Mar. 09	-2.67	-1.73	-1.07	-0.91	-1.27	-0.61	-2.19
		May 09	-1.92	-1.55	-1.30	-1.29	-1.44	-0.81	-1.50
		Mar. 10	-2.70	-0.70	-1.54	-1.14	-1.09	-0.66	-1.90
		Feb. 11	-3.37	0.26	-2.06	-1.03	-1.51	-0.09	-2.57
		Jul. 09	-2.43	-1.83	-0.01	-0.51	-3.91	-3.07	-1.91
		Aug. 09	-1.23	-0.73	-0.39	-0.19	-3.20	-1.81	-2.40
		Aug. 10	-0.66	-2.54	-0.87	-2.28	-0.85	-2.27	-0.62
S3	Monsoon	Nov. 09	-2.81	-0.71	-2.32	-1.01	-1.76	-0.65	-0.75
		Dec. 09	-2.44	-1.42	-1.28	-1.19	-1.07	-0.93	-1.54
		Dec. 10	-9.67	-7.78	-0.73	-1.08	-1.64	-0.31	-1.94
		Mar. 09	-4.04	-1.35	-1.59	-1.17	-0.99	-0.44	-1.97
		May 09	-1.20	-1.00	-0.80	-0.76	-0.39	-0.13	-1.00
		Mar. 10	-1.40	-1.12	-1.16	-1.01	-0.70	-1.25	-1.02
		Feb. 11	-1.41	-1.53	-1.00	-1.61	-0.33	-0.36	-1.16
S4	Post monsoon	Mar. 11	-1.28	-0.95	-0.78	-0.68	-0.96	-0.65	-1.06
		Jul. 09	-2.25	-2.15	-1.56	-0.67	-3.83	-1.96	-1.03
		Aug. 09	-1.19	-1.00	-0.61	-0.15	-4.57	-3.30	-1.70
		Aug. 10	-0.62	-0.85	-0.54	-0.93	-0.85	-0.65	-0.76
		Nov. 09	-1.26	-0.78	-0.56	-1.10	-0.33	-0.60	-0.82
		Dec. 09	-1.25	-1.42	-0.85	-1.21	-0.48	-0.85	-0.71
		Oct. 10	-2.29	-1.19	-1.40	-1.83	-0.87	-0.23	-1.71
S4	Premonsoon	Dec. 10	-8.49	-7.92	-1.12	-1.34	-0.60	-0.62	-1.27
		Mar. 09	-2.92	-0.42	-1.24	-0.53	-1.50	-0.18	-2.58
		May 09	-1.29	-1.65	-1.08	-1.13	-0.41	-0.42	-1.19
		Mar. 10	-1.94	0.16	-1.28	-0.19	-1.01	-0.18	-1.48
		Apr. 10	-0.66	-0.99	-0.50	-0.57	-1.11	-1.06	-0.87
		Feb. 11	-1.93	-0.46	-1.69	-0.75	-0.49	0.14	-1.41

Table 13 (continued)

Location	Season	Period	Cu	Ni		Co		Zn		Pb		Cr		Cd	
				Bulk	-63 µm										
Monsoon	Jul. 09	-2.16	-2.24	-0.64	-0.79	-1.89	-2.01	-0.91	0.60	-1.00	-1.10	0.04	-0.18	-0.58	-0.17
	Aug. 09	-1.95	-1.76	-0.76	-0.49	-2.20	-1.30	-1.64	0.41	-2.06	-0.73	-0.95	-0.37	-2.17	0.42
	Aug. 10	-1.50	-1.66	-1.46	-1.80	-1.39	-1.77	-1.27	-1.50	-0.57	-0.39	-0.21	-0.54	-0.50	-0.04
Post monsoon	Nov. 09	-1.09	-0.64	-0.66	-0.82	-0.65	-0.43	-0.65	-0.33	-0.82	-1.02	0.11	0.00	1.15	0.83

NA Not Available

concentration maps depict similar pattern with that of pollution load index.

Generally, sandy soils are rapidly permeable and tend to be low in organic matter content, low in ability to retain moisture and nutrients, in cation exchange, and buffer capacities. Sandy soils usually have high bulk densities. As the relative percentages of silt and/or clay particles become greater, the properties of soils are increasingly affected. Finer-textured soil/sediment with silt/clay, generally containing more organic matter, has higher cation exchange and buffer capacities and better able to retain moisture and nutrients. The original classification scheme developed by Shepard (1954) used for marine sediments to interpret particle size distribution to figure out sediment texture is shown for the Dhamra estuary sediments. Figure 5 represents the ternary diagram for different grain sizes at different locations combining the average of three seasons' data. It can be seen that mostly the samples are concentrated in clayey silt region which is the classified as sediment type for accumulation of metals.

In sediments, trace metal concentrations are considered to vary with sediment properties such as the percentage of OC, grain size, and Fe-Mn oxyhydroxide content (Adriano 2001). These characteristics provide a means for pollution assessment emanating from transport and deposition of the sediments. Organic carbon ranges from 0.01 to 4.97 % over the study area for the study period (Table 4). In general, the percentage of OC is found to be higher in premonsoon than post monsoon, which is found to be higher than monsoon season. The finding of organic carbon also supplements the metal pollution and its association in marine sediments.

Multivariate analysis for source apportionment in marine sediments

Out of all the variables, three principal components were extracted accounting over 66 % of the total variance. The components were ranked by the eigenvalues. In the first principal component (PC1), the metals, viz., Cd, Cr, Cu, Mn, Pb, and Co are closely associated, explaining over 26 % of total variance (Table 5). These metals are toxic metals and mostly found in mining areas, which can be considered as a point source of pollution. This may also indicate the influence of the geochemical processes and hydrodynamic behavior attributing to chromite mining activities in the near by bank of Brahmani River. It could also be an evidence of reactive

Table 14 (continued)

Location	Season	Period	Fe		Mn		Ca		Mg		Na		K	
			Bulk	-63 µm	Bulk	-63 µm	Bulk	-63 µm	Bulk	-63 µm	Bulk	-63 µm	Bulk	-63 µm
S6	Post monsoon	Nov. 09	-0.46	-0.42	-1.38	-1.38	-2.59	-2.66	-0.17	-0.33	0.25	-0.22	-1.32	-1.30
		Dec. 09	-0.52	-0.30	-1.24	-1.09	-2.17	-2.78	0.00	-0.32	0.67	-0.23	-0.84	-0.84
		Oct. 10	-0.72	-0.82	-0.36	-0.25	-2.86	-2.26	-0.55	-2.30	-0.59	-0.46	-1.69	-1.16
		Dec. 10	-0.92	-0.49	-0.95	-0.41	-3.01	-3.28	-0.92	-0.57	-0.10	-2.62	-1.87	-1.83
		Mar. 09	-2.21	-0.19	-2.91	0.17	-9.37	-8.89	-0.85	-1.81	-0.60	-1.39	-2.66	-3.60
	Premonsoon	May 09	-0.70	-0.69	0.37	0.10	-4.33	-5.22	-1.16	-0.86	-0.47	-0.83	-2.62	-2.20
		Mar. 10	-0.87	-0.24	-0.95	-0.93	-2.23	-2.07	-0.32	-0.42	0.72	-0.09	-0.67	-1.21
		Apr. 10	NA	0.40	-1.82	0.38	-2.66	-2.01	-1.97	-0.32	-0.18	-0.02	-1.24	-1.41
		Mar. 11	-1.03	-0.14	5.59	5.76	NA	NA	NA	NA	0.60	-0.98	-2.15	-2.58
		Monsoon	Jul. 09	-0.67	-0.48	-0.69	-0.69	-4.24	-3.28	-1.48	-1.89	1.77	-0.70	-1.59
	Post monsoon	Aug. 10	-1.16	-1.04	-1.67	-1.67	-2.88	-2.88	-0.48	-0.48	-3.58	-3.71	-4.83	-4.83
		Nov. 09	-0.66	-0.54	-1.24	-1.32	-2.29	-1.79	-0.23	-0.04	0.27	-0.24	-1.28	-1.19
		Dec. 09	-0.36	1.26	-0.93	-1.14	-2.52	-2.58	-0.10	-0.02	0.96	-0.01	-0.68	-0.71
S7	Premonsoon	Oct. 10	-1.33	-0.94	-1.32	-0.12	-2.98	-2.48	-0.32	-2.42	-0.27	-0.10	-1.58	-1.28
		Apr. 10	-1.52	-1.02	-1.32	-1.19	-1.68	-1.66	-0.08	-0.21	0.19	-0.06	-1.46	-1.20
		Monsoon	Jul. 09	-0.74	-0.61	-0.71	-0.69	-4.49	-3.38	-1.48	-1.44	1.28	-0.73	-1.49
S8	Post monsoon	Aug. 10	-0.71	-0.75	-1.35	-1.67	-2.85	-2.88	-0.53	-0.48	-3.47	-3.85	-4.83	-4.83
		Nov. 09	-0.46	0.64	-1.16	-1.19	-2.43	-2.19	-0.14	-0.18	0.28	-0.21	-1.38	-1.30
		Mar. 10	-0.59	0.68	-0.99	-0.84	-2.04	-2.09	-0.04	0.06	1.06	-0.01	-0.71	-1.17
	Premonsoon	Jul. 09	-0.51	-0.79	-0.78	-0.80	-4.11	-3.01	-1.25	-1.46	1.31	-0.72	-1.38	-1.52
		Aug. 09	-2.48	-1.24	-1.57	-0.93	-3.52	-3.41	-2.31	-1.62	1.80	-0.92	-1.92	-0.49
	Post monsoon	Aug. 10	-0.77	-1.03	-1.67	-1.67	-2.85	-2.85	-0.58	-0.76	-3.47	-3.71	-4.64	-4.83
		Nov. 09	-0.36	-0.26	-0.89	-1.11	-2.64	-2.59	-0.08	-0.35	0.39	-0.22	-1.06	-1.29

NA Not Available

dispersive phenomena caused by the weathering of primary minerals in sediments and subsequent transportation of contaminants in river water (Navarro and Cardellachand 2009). Fe and Mn oxyhydroxide precipitation and its scavenging effects on metals also control the mobility of metal contents in water (Schurch et al. 2004). In the second principal component (PC2), metals, viz., K, Ca, Mg, and Co are closely associated over 23 % of total variance. This may be attributed to more than one source, viz., salinization, weathering of basic rock, or mineralization causing geogenic contamination followed by run-off water in adjoining areas of the river originating from the use of manure to improve soil fertility.

Correlation and metal enrichment

The correlation coefficient between pairs of metal concentrations shows that there is a strong correlation between parameters viz., Cr versus Mn ($r=0.60$) and Cr versus Cu ($r=0.62$) (Table 6). This is an indicative of significant source of contamination attributing to chromite

mining activity with manganese oxide ores. Similarly, it is shown that correlations of Cr versus Cd ($r=0.89$), Cu versus Cd ($r=0.73$), and Cu versus Pb ($r=0.73$) in the sediment indicate their existence and similarity among them reflecting a common source of origin (Turner 2000).

Environmental significance in marine sediments

For various metals, EF, CF, PLI, and geoaccumulation index have been calculated to assess whether the concentration of metals attains contamination level or can be considered as pristine. It has been found that Cu, Ni, Pb, Zn, Cr, and Cd are moderately enriched in the sediments whereas Cr and Cd are highly enriched in the sediments in the study area irrespective of the seasonal variations (Tables 7 and 8). As far as the contamination factor is concerned, marine sediments are less contaminated by all other metals except Pb, Zn, Cr, and Cd. Among these, marine sediments are moderately contaminated by Pb and Zn in the premonsoon season. Similarly, marine sediments are considerably

contaminated by Cd but highly contaminated by Cr during premonsoon season (Tables 9 and 10). The estimation of pollution load index indicates that in the monsoon season the study area attains perfection but deteriorates the site quality during premonsoon season than in the post monsoon season (Tables 11 and 12) (Figs. 6 and 7). Elevated I_{geo} values are found for Cr in the study area which indicates that surface sediments are strongly to extremely polluted. The I_{geo} value for Cd showed that sediment is moderately to strongly polluted over the study area (Tables 13 and 14). During the investigation of the degree of pollution in surface sediments of near and offshore regions of Dhamra estuarine region based upon various established methods, it has been found that there is substantial pollution load specifically with respect to Cr and Cd derived from values estimated based upon established factors and indices. The sources are attributed to many geogenic as well as anthropogenic aspects such as nearby fishing activity, shipping activities, and contaminants transported by the run-off water of Brahmani River.

Conclusion

The overall objective of the study was to assess marine sediment pollution based upon established index estimation methods in a geospatial environment indicating the plausible sources. In order to achieve the health of marine ecosystem, the integration of geospatial technologies with analytical results is immensely essential to analyze the spatial distribution of trace and major metal concentrations in marine sediments by slicing into different pollution thresholds and understanding their influencing factors in the marine environment to eradicate and take necessary measures. The spatial distribution of metal contents in surface sediments in Dhamra estuary has been examined, which enhances the spatial data inventory to characterize the biogeochemical processes in the surface sediments in this tropical estuarine system. The comparison of spatial pattern in distribution of metals indicates that there is substantial pollution. The pollution impact was assessed by means of estimation of enrichment factor, contamination factor, pollution load index, and geoaccumulation index which are very much useful to derive a conclusion about the pollution level in the study area. The correlation study with organic carbon helped in better understanding of the distribution of metals and its association. The values

from calculation of EF, CF, and I_{geo} indicate that there is Cr enrichment in sediments attributing to its sources, anthropogenic as well as geogenic contamination of Cr through Brahmani River from chromite ore mines in Sukinda valley. Values of PLI indicate that sediment quality is deteriorated during premonsoon season. Multivariate statistical analysis i.e., principal component analysis, was found to be a very useful tool to pinpoint plausible sources of contaminants. The elevated Cr in marine sediment comes from natural and anthropogenic sources. The current study ascertains the effect of geogenic/anthropogenic impact in the Dhamra estuary on the east coast of India, as the increasing mining activities influence the geochemical process in the estuarine systems.

Acknowledgments The authors would like to thank Prof. (Dr.) B. K. Mishra, Director, Institute of Minerals and Materials Technology (IMMT) for his constant guidance, encouragement, and motivation in working and disseminating. The financial grant from the Dhamra Port Corporation Limited (DPCL), Government of India is gratefully acknowledged. Thanks are also extended to all the project personnel who have provided technical and operational assistance in the collection and analysis of samples during the monitoring program.

References

- Adriano, D. C. (2001). *Trace metals in terrestrial environments: biogeochemistry, bioavailability and risks of metals*. New York: Springer.
- Aksu, A. E., Yasar, D., & Uslu, O. (1998). Assessment of marine pollution in Izmir Bay: heavy metal and organic compound concentrations in surficial sediments. *Turkish Journal of Engineering and Environmental Sciences*, 22, 387–415.
- Attea, O., Dubois, J. P., & Webster, R. (1994). Geostatistical analysis of soil contamination in the Swiss Jura. *Environmental Pollution*, 86, 315–327.
- Beiras, R., Bellas, J., Fernández, N., Lorenzo, J. I., & Cobela-García, A. (2003). Assessment of coastal marine pollution in Galicia (NW Iberian Peninsula); metal concentrations in seawater, sediments and mussels (*Mytilus galloprovincialis*) versus embryo-larval bioassays using *Paracentrotus lividus* and *Ciona intestinalis*. *Marine Environmental Research*, 56, 531–553.
- Buat-Menard, P., & Chesselet, R. (1979). Variable influence of the atmospheric flux on the trace metal chemistry of oceanic suspended matter. *Earth Planet Science Letter*, 42, 398–411.
- Bustard, H. R., & Kar, S. (1981). Annual nesting of the Pacific ridley sea turtle (*Lepidochelys olivacea*) in Odisha, India. *British Journal of Herpetology*, 6, 139.

- Caccia, V. G., Millero, F. J., & Palanques, A. (2003). The distribution of trace metals in Florida Bay sediments. *Marine Pollution Bulletin*, 46, 1420–1433.
- Calvert, S., & Pedersen, T. (1993). Geochemistry of recent oxic and anoxic marine sediments: implications for the geological records. *Marine Geology*, 11, 67–88.
- Chakravarty, M., & Patgiri, A. D. (2009). Metal pollution assessment in sediments of the Dikrong River, NE India. *Journal of Human Ecology*, 27, 63–67.
- Dash, M. C., & Kar, C. S. (1990). *The turtle paradise, Gahirmatha: an ecological analysis and conservation strategy* (pp. 1–295). New Delhi: Interprint press.
- Dekov, V. M., Subramanian, V., Van Grieken, R., (1999). Chemical composition of riverine suspended matter and sediments from the Indian sub-continent. In V. Ittekot, V. Subramanian, & S. Annadurai (Eds.), *Biogeochemistry of rivers in tropical South and Southeast Asia. Heft 82, SCOPE Sonderband, Mitteilungen aus dem Geologisch-Paläontologischen* (pp. 99–109). Institut der Universität: Hamburg.
- Einax, J. W., Zwanzinger, H. W., & Geib, S. (1997). *Chemometrics in environmental analysis*. Weinheim: Wiley-VCH.
- Elsdon, T. S., & Connell, S. D. (2009). Spatial and temporal monitoring of coastal water quality: refining the way we consider, gather, and interpret patterns. *Aquatic Biology*, 5, 157–166.
- El Nemr, A., Khaled, A., & Sikaily, A. E. (2006). Distribution and statistical analysis of leachable and total heavy metals in the sediments of the Suez Gulf. *Environmental Monitoring and Assessment*, 118, 89–112.
- Facchinelli, A., Sacchi, E., & Mallen, L. (2001). Multivariate statistical and GIS-based approach to identify heavy metal sources in soils. *Environmental Pollution*, 114, 245–276.
- Flanagan, F. J. (1973). 1972 values for international geochemical reference samples. *Geochimica Cosmochimica Acta*, 37, 1189–1200.
- Gaudette, H. E., Flight, W. R., Toner, L., & Folger, D. W. (1974). An inexpensive titration method for the detection of organic carbon in recent sediments. *Journal of Sediment Petrology*, 44, 249–253.
- Hakanson, L. (1980). Ecological risk index for aquatic pollution control, a sedimentological approach. *Water Research*, 14, 975–1001.
- Harbison, P. (1984). Regional variation in the distribution of trace metals in modern intertidal sediments of northern Spencer Gulf, South Australia. *Marine Geology*, 61, 221–247.
- Lewis, D. W. (1984). *Practical sedimentology* (p. 227). Pennsylvania: Hutchinson Ross Publishing Company.
- Muller, G. (1969). Index of Geoaccumulation in the sediments of the Rhine River. *Geojournal*, 2, 108–118.
- Nasr, M. S., Okbah, M. A., & Kasem, S. M. (2006). Environmental assessment of heavy metal pollution in bottom sediment of Aden port, Yemen. *International Journal of Oceans and Oceanography*, 1, 99–109.
- Navarro, A., & Cardellachand, E. (2009). Mobilization of Ag, heavy metals and Eu from the waste deposit of the Las Herrerías mine (Almería, SE Spain). *Environmental Geology*, 56(7), 1389–1404.
- O'Regan, P. R. (1996). The use of contemporary information technologies for coastal research and management - a review. *Journal of Coastal Research*, 12, 192–204.
- Pekey, H. (2006). Heavy metals pollution assessment in sediments of the Izmit Bay, Turkey. *Environmental Monitoring and Assessment*, 123, 219–231.
- Ravichandran, M., Baskaran, M., Santschi, P. H., & Bianchi, T. (1995). History of trace metal pollution in Sabine-Neches Estuary, Beaumont, Texas. *Environmental Science and Technology*, 29, 1495–1503.
- Richard, R., Rendigs, M., & Bothner, H. (2001). United States of Geological Survey Report, 01–499.
- Ridgway, J., & Shimmield, G. (2002). Estuaries as repositories of historical contamination and their impact on shelf seas. *Estuarine, Coastal and Shelf Science*, 55, 903–928.
- Riley, J. P., & Chester, R. (1971). *An introduction to marine chemistry*. London: Academic.
- Roy, S., & Katpatal, Y. B. (2011). Cyclical hierarchical modeling for water quality model-based DSS module in an urban river system. *Journal of Environmental Engineering*, 137(12), 1176–1184.
- Salomons, W., & Forstner, U. (1984). *Metals in hydrocycle* (pp. 63–98). Berlin: Springer.
- Satapathy, D. R., Salve, P. R., & Katpatal, Y. B. (2009). Spatial distribution of metals in ground/surface waters in the Chandrapur district (Central India) and their plausible sources. *Environmental Geology*, 56, 1323–1352.
- Schurch, M., Edmunds, W. M., & Buckley, D. (2004). Three-dimensional flow and trace metal mobility in shallow Chalk groundwater, Dorset, United Kingdom. *Journal of Hydrology*, 292(1–4), 229–248.
- Seshan, B. R. R., Natesan, U., & Deepthi, K. (2010). Geochemical and statistical approach for evaluation of heavy metal pollution in core sediments in southeast coast of India. *International Journal of Environmental Science and Technology*, 7, 291–306.
- Sharma, V. K., Rhudy, K. B., Koenig, R., Baggett, A. T., Hollyfield, S., & Vazquez, F. G. (1999). Metals in sediments of Texas estuaries, USA. *Journal of Environmental Science and Health*, 34, 2061–2073.
- Shepard, F. P. (1954). Nomenclature based on sand-silt-clay ratios. *Journal of Sedimentary Petrology*, 24, 151–158.
- Simex, S. A., & Helz, G. R. (1981). Regional geochemistry of trace elements in Chesapeake Bay. *Environmental Geology*, 3, 315–323.
- Stanbury, K. B., & Starr, R. M. (1999). Applications of Geographic Information Systems (GIS) to habitat assessment and marine resource management. *Oceanologica Acta*, 22, 699–703.
- Sutherland, R. A. (2000). Bed sediment-associated trace metals in an urban stream, Oahu, Hawaii. *Environmental Geology*, 39, 611–627.
- Tao, S. (1995). Kriging and mapping of copper, lead and mercury contents in surface soil in Shenzhen area. *Water Air Soil Pollution*, 83, 161–172.
- Tessier, A., Campbell, P. G. C., & Bisson, M. (1979). Sequential extraction procedures for the speciation of particulate trace metals. *Analytical Chemistry*, 51, 844–851.
- Tomlinson, D. L., Wilson, J. G., Harris, C. R., & Jeffney, D. W. (1980). Problems in the assessment of heavy metal levels in estuaries and the formation of a pollution index. *Helgoländer Wissenschaftliche Meeresuntersuchungen*, 33, 566–572.

- Tuncer, G., Tunç, G., & Balkaş, T. I. (2001). Evolution of metal pollution in the golden horn (Turkey) sediments between 1912 and 1987. *Marine Pollution Bulletin*, 5, 350–360.
- Turekian, K. K., & Wedepohl, K. H. (1961). Distribution of the elements in some major units of the earth's crust. *Bulletin Geological Society of America*, 72, 175–192.
- Turner, A. (2000). Trace metal concentration in sediments from U.K. Estuaries: an empirical evaluation of the role of hydrous iron and manganese oxides. *Estuarine, Coastal and Shelf Science*, 50, 355–371.
- Vazquez, F. G., & Sharma, V. K. (2004). Major and trace elements in sediments of the Campeche Sound, southeast Gulf of Mexico. *Marine Pollution Bulletin*, 48, 87–90.
- Wang, F. H. (2006). *Quantitative methods and applications in GIS*. New York: Taylor & Francis.
- Wentworth, C. K. (1922). A scale of grade and class terms for elasic sediments. *Journal of Geology*, 30, 377–392.
- Wiechula, L., Loska, K., & Wiechula, D. (2003). Application of principal component analysis for the estimation of source of heavy metal contamination in surface sediments from the Rybník Reservoir. *Chemosphere*, 51, 723–733.
- Wolanski, E. (2007). *Estuarine ecohydrology*. Amsterdam: Elsevier. ISBN 978-0-444-53066-0.
- Zhou, F., Guo, H. C., & Liu, L. (2007). Quantitative identification and source apportionment of anthropogenic heavy metals in marine sediment of Hong Kong. *Environmental Geology*, 53(2), 295–305.